

DTIC FILE COPY

4

AD-A216 999

AFGL-TR-89-0030  
AIR FORCE SURVEYS IN GEOPHYSICS, NO. 451

A Three-Component Seismic Refraction  
Survey in Northwestern Arizona

VIVIAN K. HUSSEY



31 January 1989



Approved for public release; distribution unlimited.



EARTH SCIENCES DIVISION

AIR FORCE GEOPHYSICS LABORATORY

HANSCOM AFB, MA 01731

DTIC  
ELECTE  
JAN 19 1990  
S B D

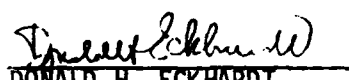
PROJECT 2309

90 01 19 013

"This technical report has been reviewed and is approved for publication"

FOR THE COMMANDER

  
HENRY A. OSSING, Chief  
Solid Earth Geophysics Branch

  
DONALD H. ECKHARDT  
Director  
Earth Sciences Division

This report has been reviewed by the ESD Public Affairs Office (PA) and is releasable to the National Technical Information Service (NTIS).

Qualified requestors may obtain additional copies from the Defense Technical Information Center. All others should apply to the National Technical Information Service.

If your address has changed, or if you wish to be removed from the mailing list, or if the addressee is no longer employed by your organization, please notify GL/IMA, Hanscom AFB, MA 01731. This will assist us in maintaining a current mailing list.

Do not return copies of this report unless contractual obligations or notices on a specific document requires that it be returned.

UNCLASSIFIED

SECURITY CLASSIFICATION OF THIS PAGE

| REPORT DOCUMENTATION PAGE  |       |   |   | Form Approved<br>OMB No. 0704-016                        |                                |
|--|-------|---|---|--|--------------------------------|
| 1a. REPORT SECURITY CLASSIFICATION<br>Unclassified   |       |   | 1b. RESTRICTIVE MARKINGS  |  |                                |
| 2a. SECURITY CLASSIFICATION AUTHORITY  |       |   | 3. DISTRIBUTION / AVAILABILITY OF REPORT<br>Approved for public release;<br>distribution unlimited. |  |                                |
| 2b. DECLASSIFICATION / DOWNGRADING SCHEDULE  |       |   |   |  |                                |
| 4. PERFORMING ORGANIZATION REPORT NUMBER(S)<br>AFGL-TR-89-0030<br>AFSG, No. 451  |       |   | 5. MONITORING ORGANIZATION REPORT NUMBER(S)   |  |                                |
| 6a. NAME OF PERFORMING ORGANIZATION<br>Air Force Geophysics<br>Laboratory  |       | 6b. OFFICE SYMBOL<br>(If applicable)<br>LWH |   | 7a. NAME OF MONITORING ORGANIZATION                      |                                |
| 6c. ADDRESS (City, State, and ZIP Code)<br>Hanscom AFB<br>Massachusetts 01731-5000   |       |   | 7b. ADDRESS (City, State, and ZIP Code)   |  |                                |
| 8a. NAME OF FUNDING / SPONSORING<br>ORGANIZATION   |       | 8b. OFFICE SYMBOL<br>(If applicable)        |   | 9. PROCUREMENT INSTRUMENT IDENTIFICATION NUMBER          |                                |
| 8c. ADDRESS (City, State, and ZIP Code)  |       |   | 10. SOURCE OF FUNDING NUMBERS   |  |                                |
|  |       |   | PROGRAM<br>ELEMENT NO.<br>61102F  | PROJECT<br>NO.<br>2309                                   | TASK<br>NO.<br>G2              |
|  |       |   | WORK UNIT<br>ACCESSION NO.<br>04  |  |                                |
| 11. TITLE (Include Security Classification)<br>A Three-Component Seismic Refraction Survey in Northwestern Arizona   |       |   |   |  |                                |
| 12. PERSONAL AUTHOR(S)<br>Hussey, V.K.   |       |   |   |  |                                |
| 13a. TYPE OF REPORT<br>Scientific, Interim   |       | 13b. TIME COVERED<br>FROM _____ TO _____    |   | 14. DATE OF REPORT (Year, Month, Day)<br>1989 January 31 |                                |
| 15. PAGE COUNT<br>56   |       |   |   |  |                                |
| 16. SUPPLEMENTARY NOTATION<br>A thesis submitted in partial fulfillment of the requirements for the<br>Degree of Master of Science at The Graduate School of Arts and Sciences, Department of<br>Geology and Geophysics, Boston College.   |       |   |   |  |                                |
| 17. COSATI CODES   |       |   | 18. SUBJECT TERMS (Continue on reverse if necessary and identify by block number)                   |  |                                |
| FIELD  | GROUP | SUB-GROUP                                   | Seismology, crustal structure, southwestern United States   |  |                                |
| 08   | 11    |   |   |  |                                |
| 19. ABSTRACT (Continue on reverse if necessary and identify by block number)   |       |   |   |  |                                |
| <p>Three-component seismic refraction data were recorded in northwestern Arizona in the Transition Zone between the Colorado Plateau and Basin and Range provinces. A 35.4 km array received shots from both these provinces. Seismograms from the southwest shots show two prominent reflections, indicating a reflector about 20 km deep and Moho depths of 26.5 - 29 km in the Basin and Range and 29 - 31 km in the Transition Zone. A weak PmP from the northeast suggests the crust or Moho in the Colorado Plateau has different characteristics than in the Basin and Range. Raytracing yields Pn and Sn velocities of 7.95 km/s and 4.59 km/s for the Transition Zone and shows evidence of laterally increasing Pn and Sn velocities toward the Basin and Range and the Colorado Plateau. Clear Pg and Sg arrivals reveal a low Poisson's ratio of 0.217 for the upper crust of the Colorado Plateau.</p> <p><i>Three-component seismic refraction data were recorded in northwestern Arizona in the Transition Zone between the Colorado Plateau and Basin and Range provinces. A 35.4 km array received shots from both these provinces. Seismograms from the southwest shots show two prominent reflections, indicating a reflector about 20 km deep and Moho depths of 26.5 - 29 km in the Basin and Range and 29 - 31 km in the Transition Zone. A weak PmP from the northeast suggests the crust or Moho in the Colorado Plateau has different characteristics than in the Basin and Range. Raytracing yields Pn and Sn velocities of 7.95 km/s and 4.59 km/s for the Transition Zone and shows evidence of laterally increasing Pn and Sn velocities toward the Basin and Range and the Colorado Plateau. Clear Pg and Sg arrivals reveal a low Poisson's ratio of 0.217 for the upper crust of the Colorado Plateau.</i></p> |       |   |   |  |                                |
| 20. DISTRIBUTION/AVAILABILITY OF ABSTRACT<br><input type="checkbox"/> UNCLASSIFIED/UNLIMITED <input type="checkbox"/> SAME AS RPT. <input checked="" type="checkbox"/> DTIC USERS  |       |   | 21. ABSTRACT SECURITY CLASSIFICATION<br>Unclassified  |  |                                |
| 22a. NAME OF RESPONSIBLE INDIVIDUAL<br>John J. Cipar   |       |   | 22b. TELEPHONE (Include Area Code)<br>617-377-3746  |  | 22c. OFFICE SYMBOL<br>AFGL/LWH |

DD FORM 1473, JUN 86

Previous editions are obsolete.

SECURITY CLASSIFICATION OF THIS PAGE

UNCLASSIFIED

## Preface

Several members of various organizations made contributions to this research project. The Air Force Geophysics Laboratory provided the data and kindly allowed me to freely use their computer and other facilities. Mary Beth Hultt, the AFGL principal investigator for the experiment, assisted in organizing pertinent information and in processing data. The data were collected by Joe Craig and Michael Hines of AFGL, Al Leverette and Robert Goerke of the Air Force Weapons Laboratory, Robert Lory of Boston College, Steve Mangino of the State University of New York, and Geoff Abers of the Massachusetts Institute of Technology in addition to Mary Beth and myself. Jill McCarthy of the United States Geologic Survey provided extensive information on the Pacific Arizona Crustal Experiment as well as the raytracing program used in the analysis.

I am grateful to my advisors, John Cipar of AFGL, and John Ebel and John Devane of Boston College, for their assistance in preparing this thesis. In addition, I thank Andrew Lazarewicz of AFGL for his continued support and technical advice.



|                           |                                     |
|---------------------------|-------------------------------------|
| <b>Accession For</b>      |                                     |
| NTIS GRA&I                | <input checked="" type="checkbox"/> |
| DTIC TAB                  | <input type="checkbox"/>            |
| Unannounced               | <input type="checkbox"/>            |
| Justification _____       |                                     |
| By _____                  |                                     |
| Distribution/ _____       |                                     |
| <b>Availability Codes</b> |                                     |
| Dist                      | Avail and/or Special                |
| A-1                       |                                     |

## Contents

|   |    |
|---|----|
| 1. INTRODUCTION                                   | 1  |
| 2. GEOLOGIC AND TECTONIC SETTING                  | 8  |
| 3. PAST SEISMIC STUDIES                           | 11 |
| 4. EXPERIMENTAL DETAILS                           | 19 |
| 5. INTERPRETATION                                 | 26 |
| 5.1 Crustal Compressional Velocity Structures     | 31 |
| 5.2 Shear Velocity Structure and Poisson's Ratios | 39 |
| 6. CONCLUSIONS                                    | 45 |
| REFERENCES  | 47 |

## Illustrations

|   |    |
|---|----|
| 1. Physiographic Map of the Western United States   | 2  |
| 2. Schematic Drawing of Locations of Seismic Studies Reviewed   | 4  |
| 3. Map of Northwestern Arizona Showing Shot Point and Station Locations                                 | 6  |
| 4. COCORP Profile in Southwestern Arizona   | 7  |
| 5. Models Presented by Warren   | 13 |
| 6. Initial Model Used for Raytracing  | 27 |
| 7. Composite Seismic Records from Shots Southwest of the Stations With a Superimposed Travel Time Curve | 29 |
| 8. Composite Seismic Records from Shots Northeast of the Stations With a Superimposed Travel Time Curve | 30 |
| 9. AFGL Model of the Southern Basin and Range, of the Transition Zone, and the Colorado Plateau         | 34 |
| 10. Cartoon Drawing of the Velocity Structure and Poisson's Ratios of the AFGL Model                    | 35 |
| 11. Raytracing from Shot Point 20 (SH15) Through the USGS Crustal Structure                             | 36 |
| 12. Raytracing from Shot Point 20 (SH15) Through the AFGL Crustal Structure                             | 38 |
| 13. Theoretical Ray Paths through the AFGL Model from Shots in the Colorado Plateau                     | 40 |
| 14. Comparison of P and S Velocities in the Upper Crust of the Colorado Plateau                         | 42 |
| 15. Comparison of P and S Velocities in the Upper Crust of the Basin and Range                          | 43 |
| 16. Comparison of P and S Velocities in the Lower Crust of the Basin and Range                          | 44 |

## Tables

|  |    |
|--|----|
| 1. Colorado Plateau Models                                       | 14 |
| a. Keller and others (1975)                                      |    |
| b. Braile and others (1974)                                      |    |
| c. Roller (1965)   |    |
| 2. Southern Basin and Range Models                               | 14 |
| a. Diment and others (1961)                                      |    |
| b. Sinno and others (1981)                                       |    |
| c. McCarthy and others (1987)                                    |    |
| d. Langston and Helmberger (1974)                                |    |
| 3. Shot Location Information                                     | 20 |
| 4. Station Location Information                                  | 21 |
| 5. Instrument Constants  | 22 |
| 6. Time Corrections  |    |
| a. First Shot Window   | 23 |
| b. Second Shot Window  | 24 |
| c. Third Shot Window   | 25 |
| 7. Velocity Information  | 33 |
| a. USGS Model Raytracing Gradients                               |    |
| b. AFGL Model Raytracing Gradients                               |    |
| c. AFGL Model Raytracing Average Velocities and Poisson's Ratios |    |

## A Three-Component Seismic Refraction Survey in Northwestern Arizona

### 1. INTRODUCTION

For many years there has been an interest in the geological processes that gave rise to the Colorado Plateau and the Basin and Range, two distinct physiographic provinces (Figure 1) in the southwestern United States. The northern Basin and Range, centered in Nevada, is characterized as having a thin crust, high heat flow (near 2 HFU; 1 HFU=43 mW/m<sup>2</sup>), extensive Cenozoic volcanism and normal faulting. The southern Basin and Range, located in southeastern California and western and southern Arizona, has similar characteristics, with the crust thinning toward the southwest away from the Transition Zone that separates the Basin and Range from the Colorado Plateau. In contrast to the Basin and Range, the Colorado Plateau, extending into parts of Utah, Colorado, Arizona, and New Mexico, is characterized by a thick crust and low heat flow (1.0 - 1.5 HFU). Late Cenozoic faulting is significantly displayed only along the western border of the relatively undeformed, but uplifted Colorado Plateau block. The Transition Zone in central Arizona has been characterized as having late Cenozoic basaltic volcanic activity.<sup>1</sup>

A recent geophysical experiment that provided an opportunity to study the transition between the two provinces was the Pacific-Arizona Crustal Experiment (PACE). PACE, sponsored by the United States Geological Survey (USGS), was designed to investigate crustal structures and processes

---

(Received for Publication 18 November 1988)

1. Sinno, Y.A., Keller, G.R., and Sbar, M.L. (1981) A Crustal Seismic Refraction Study in West-Central Arizona, *J. of Geophys. Res.* **86**(B6):5023-5038.





Figure 1. Physiographic Map of the Western United States. It is based on province divisions presented by Thompson and Zoback<sup>2</sup> and Chronic.<sup>3</sup> The Pacific-Arizona Crustal Experiment transect is within the boxed-in area through southern California and into Arizona.

2. Thompson, G.A., and Zoback, M.L. (1979) Regional Geophysics of the Colorado Plateau, *Tectonophysics* **61**:149-181.
3. Chronic, H. (1986) *Roadside Geology of Arizona*, Mountain Press Publishing Company, Missoula, MT, 340p.

across the Pacific Plate-North American Plate boundary. The area of investigation (see Figure 1) stretches 900 km across the Pacific Ocean, southern California, and into Arizona. The PACE transect cuts across the southern United States Cordillera, which includes the southern Basin and Range, the Colorado Plateau, and the Transition Zone between them.

To date the USGS has performed two vertical-component seismic refraction surveys, both of which incorporated the advantages of close station spacing and digital recorded data. In 1985, 260 km of reversed seismic refraction data were collected by the USGS in a cross-line profile located in the Whipple Mountains in southern California and western Arizona<sup>4</sup> (Figure 2). The survey revealed a crustal thickness of 26 - 27 km and an upper mantle P velocity of 7.8 km/s in the Whipple Mountain area.

The second USGS PACE seismic refraction survey was carried out in northwestern Arizona<sup>5</sup> in 1987 (Figure 2). For this USGS experiment, the USGS shot-line transected the southern Basin and Range, the Colorado Plateau, the Transition Zone, stretching from Quartzite to Camp Wood in Arizona. The records were interpreted<sup>5</sup> to yield a Moho depth of about 30 km at the southwestern end of the line and about 32 km at the northeastern end. Strong, shallow reflections were noted in the vicinity of Bagdad, Arizona, and a midcrustal layer of 22 km is reported for the southern Basin and Range and the Transition Zone. Apparent upper mantle velocities are about 7.7 km/s to the southwest and 7.9 km/s to the northeast.

In addition to the USGS refraction surveys, the 6 - 8 year PACE plan consists of coordinated multidisciplinary geophysical and geological studies and was designed to coincide with California Consortium for Crustal Studies (CALCRUST) and Consortium for Continental Reflection Profiling (COCORP) seismic reflection studies carried out within the PACE transect. CALCRUST collected seismic reflection data near the USGS seismic refraction experiment in the area of the Whipple and Buckskin Mountains in 1985. Portions of the Whipple detachment fault were imaged as a result of the profile, aiding in the USGS refraction interpretation. CALCRUST also contributed personnel and field resources to a multichannel experiment by Stanford University recorded piggyback from the 1987 USGS PACE shots. In addition, CALCRUST is working with USGS PACE scientists at Flagstaff on the geologic interpretation of industry seismic profiles collected in the Transition Zone and the southern Basin and Range. Joint interpretation of reprocessed CALCRUST seismic profiles of Chuckwalla Valley, California is underway in Menlo Park, California by USGS and CALCRUST scientists.

Two reflection surveys have been performed by COCORP within the PACE Transect (Figure 2). Strong reflections were recorded in the southern Basin and Range revealing complex shallow layering up to 15 - 18 km deep (5 - 6 seconds two-way travel time) and possible offsets in the Moho in the

- 
4. McCarthy, J., Fuis, G.S., and Wilson, J. (1987) Crustal Structure of the Whipple Mountains, Southeastern California: A Refraction Study Across a Region of Large Continental Extension, *Geophys. J.R. Astr. Soc.* **89**:119-124.
  5. McCarthy, J., Fuis, G.S., Wilson, J., McKissick, C., and Larkin, S. (1987) Pace Seismic Refraction and Wide-Angle Reflection Data Recorded Across the Central Arizona Transition Zone, *EOS Transactions* **68**(44):1359.

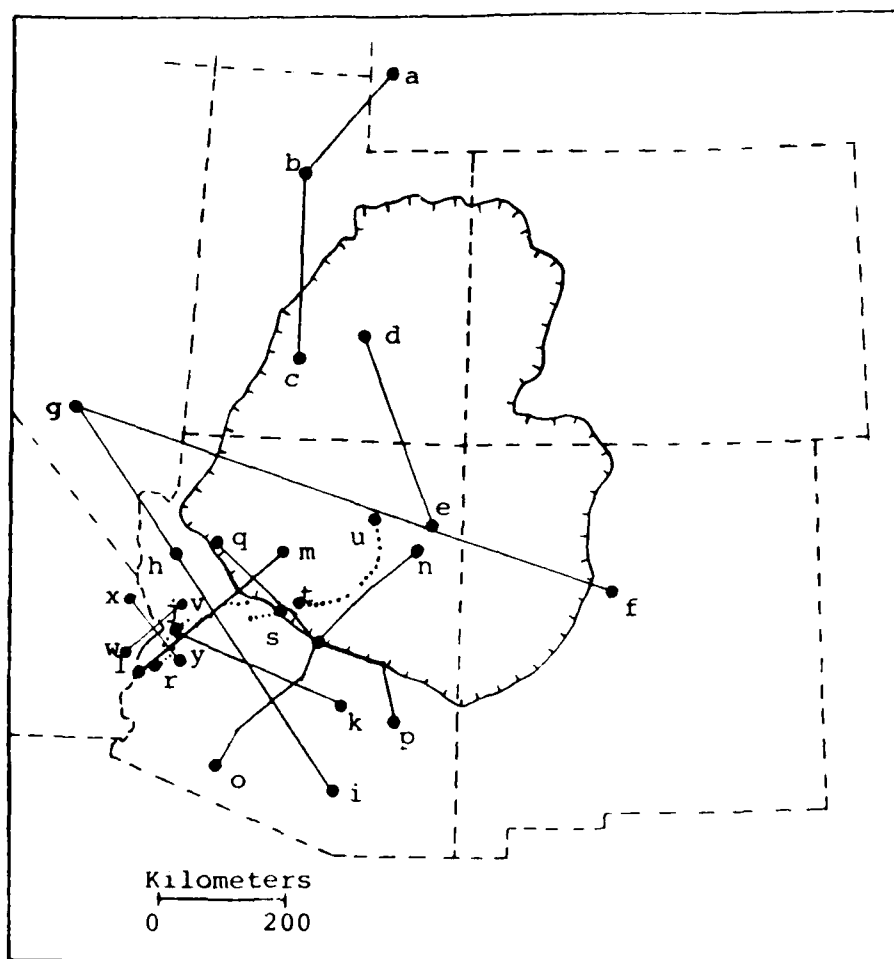


Figure 2. Schematic Drawing of Locations of Seismic Studies Reviewed. Dotted lines indicate reflection lines. The Colorado Plateau is within the hatched line. ab: Braille and others<sup>6</sup>; bc: Keller and others<sup>7</sup>; de: Roller<sup>8</sup>; fghi: Bache and others<sup>9</sup>; ghi: Langston and Helmberger<sup>10</sup>; jk: Sinno and others<sup>1</sup>; gh: Diment and others<sup>11</sup>; lm: McCarthy and others<sup>3</sup>, and present study; no and pq: Warren<sup>12</sup>; rs: Hauser and others<sup>13</sup>; tu: Hauser and Lundy<sup>14</sup>; vw and xy: McCarthy and others.<sup>2</sup> Compiled from Sinno and others<sup>1</sup>, Hauser and others<sup>13</sup>, Hauser and Lundy<sup>14</sup>, and McCarthy and others.<sup>2</sup>

Transition Zone.<sup>13</sup> The Colorado Plateau records do not reveal strong reflections, although they do indicate a depth to the Moho discontinuity of 50 km<sup>14</sup>, 8 - 10 km deeper than was previously published.<sup>8,12</sup>

This particular study is based on an Air Force Geophysics Laboratory (AFGL) crustal seismic refraction data set recorded piggyback from the PACE 1987 seismic refraction survey. The data were collected cooperatively by the Air Force Geophysics Laboratory, the Air Force Weapons Laboratory, Boston College, State University of New York, and Massachusetts Institute of Technology. Throughout this report, these data will be referred to as AFGL data. The 35.4 km AFGL line of three-component 1 and 2 Hz seismometers was placed at the northeast end of the USGS PACE line in northwestern Arizona (Figure 3). The AFGL station line, located between Bagdad and Camp Wood, Arizona, was entirely within the Transition Zone. Most of the AFGL stations were coincident with the vertical-component USGS stations. However, the AFGL station spacing was about 1.5 km in comparison to 0.75 km for USGS stations. PACE shots were received by the AFGL recorders from the Colorado Plateau and from the southern Basin and Range permitting a sampling of the crust beneath both of those provinces as well as from the Transition Zone. In addition, the AFGL instrument placement between the two towns of Bagdad and Camp Wood instrumented a gap in recent COCORP line data<sup>13</sup> (Figure 4).

The primary purpose of this particular study was to use the horizontal-component data collected by AFGL to develop, through raytracing, shear-wave velocity structures for the southern Basin and Range, the Colorado Plateau, and the Transition Zone. The initial model employed in the raytracing

- 
6. Braile, L.W., Smith, R.B., Keller, G.R., and Welch, R.M. (1974) Crustal Structure Across the Wasatch Front from Detailed Seismic Refraction Studies, *J. of Geophys. Res.* **79**(17):2669-2677.
  7. Keller, G.R., Smith, R.B., and Braile, L.W. (1975) Crustal Structure Along the Great Basin-Colorado Plateau Transition from Seismic Refraction Studies, *J. of Geophys. Res.* **80**:1093-1098.
  8. Roller, J.C. (1965) Crustal Structure in the Eastern Colorado Plateaus Province from Seismic-Refraction Measurements, *Bull. of the Seismolog. Soc. of Amer.* **55**(No. 1):107-119.
  9. Bache, T.C., Rodi, W.L., and Harkrider, D.G. (1978) Crustal Structures Inferred from Rayleigh-Wave Signatures of NTS Explosions, *Bull. of the Seismolog. Soc. of Amer.* **68**(No. 5):1399-1413.
  10. Langston, C.A. and Helmberger, D.V. (1974) Interpretation of Body and Rayleigh Waves from NTS to Tucson, *Bull. of Seismolog. Soc. of Amer.* **64**(6):1919-1929.
  11. Diment, W.H., Stewart, S.W., and Roller, J.C. (1961) Crustal Structure from the Nevada Test Site to Kingman, Arizona, from Seismic and Gravity Observations, *J. of Geophys. Res.* **66**(1):201-213.
  12. Warren, D.H. (1969) A Seismic-Refraction Survey of Crustal Structure in Central Arizona, *Geolog. Soc. of Amer. Bull.* **80**:257-282.
  13. Hauser, E.C., Gephart, J., Latham, T., Oliver, J., Kaufman, S., Brown, L., and Lucchitta, I. (1987) COCORP Arizona Transect: Strong Crustal Reflections and Offset Moho Beneath the Transition Zone, *Geology* **15**:1103-1106.
  14. Hauser, E.C. and Lundy (1988) COCORP Deep Reflections: Moho at 50 km (16 s) Beneath the Colorado Plateau, in review for *J. of Geophys. Res.*

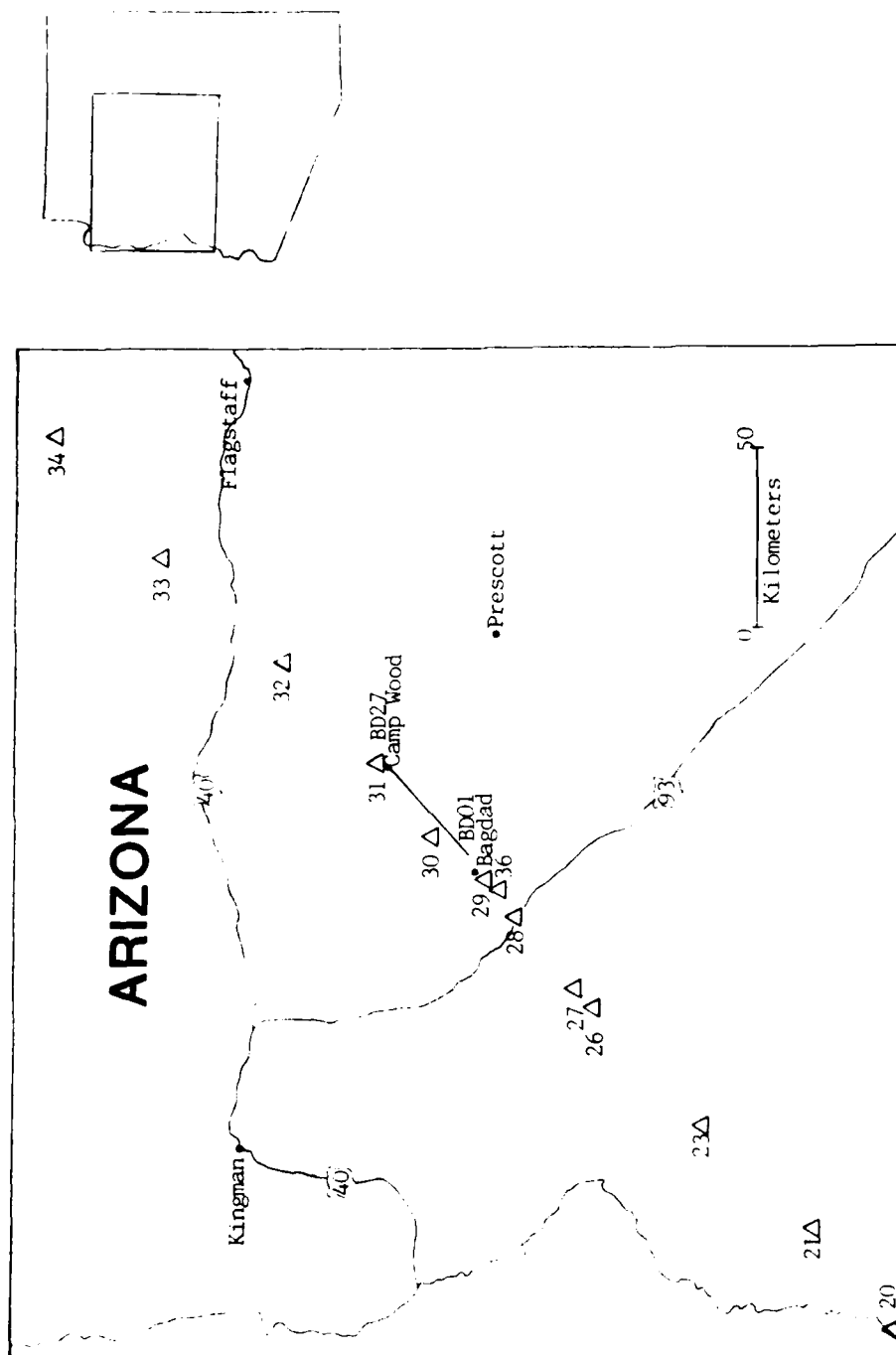


Figure 3. Map of Northwestern Arizona Showing Shot Point and Station Locations. Shot points are indicated by triangles. Stations L001 to BD27 were located along the line between Bagdad and Camp Wood.

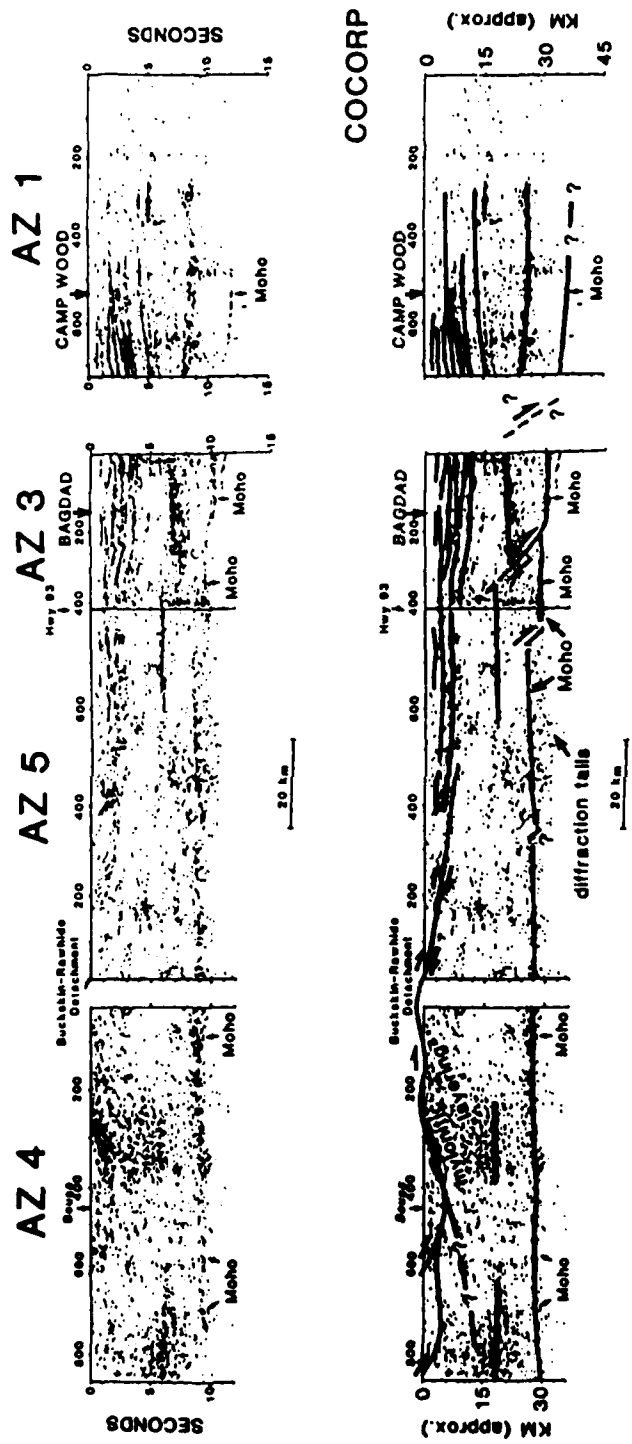


Figure 4. COCORP Profile in Southwestern Arizona. The Air Force Geophysics Laboratory seismic refraction line was placed between Bagdad and Camp Wood, Arizona, within a gap in the COCORP seismic reflection line. The COCORP profile shown above, suggests numerous shallow reflective surfaces in the Transition Zone, which is located to the right of Highway 93. Offsets in the Moho and an anticlinal feature west of Bagdad are also inferred (Modified from Hauser and others. 13)

analysis, provided by the USGS, was developed by them as a result of a raytracing analysis of the USGS 1987 PACE seismic refraction survey.<sup>3</sup> In this study the USGS model was first tested by raytracing with the AFGL vertical-component, compressional-wave arrival times. After a few adjustments, crustal P velocity models were developed from the AFGL data. Then, the AFGL horizontal-component, shear arrival times were used in a raytracing analysis to develop the shear-wave velocity structure. Finally, the compressional and shear velocity structures developed using the AFGL data were used to calculate Poisson's ratios for the crustal structures of the Basin and Range, the Colorado Plateau, and the Transitional Zone.

## 2. GEOLOGIC AND TECTONIC SETTING

The geologic and tectonic setting of the Basin and Range and the Colorado Plateau Provinces stems from a complex series of events that occurred throughout the Western United States. The earliest rocks underlying the interior of the Western United States are Precambrian metamorphic rocks formed in the Hudsonian Orogeny (1,800 million years ago).<sup>15</sup> Metamorphic and intrusive rocks found in the Basin and Range are of Elsonian (1,500 to 1,300 million years ago) and Grenville (about 1,000 million years ago) age.<sup>16</sup>

The feature that dominated the tectonic framework of the western United States during late Precambrian and Paleozoic time<sup>17</sup> was the Cordilleran Geosyncline<sup>18,19</sup>, which was well developed by latest Precambrian.<sup>20</sup> The geosyncline is made up of deposits formed all along the continental margin of North America. Late Precambrian deposits also collected further west in back-arc basins and on island arcs.<sup>21</sup>

During the Paleozoic (about 550 - 240 million years ago), the interior of the western United States, between what is now the Basin and Range and the Rocky Mountains, was a broad craton covered with a relatively thin veneer of Paleozoic rocks.<sup>16</sup> The Cordilleran miogeosyncline stretched

- 
15. King, P.B. (1969) The tectonics of North America - A Discussion to Accompany the Tectonic Map of North America, scale 1:5,000,000: U.S. Geological Survey Prof. Paper 268, 95p.
  16. Stewart, J.H. (1978) Basin-Range Structure in Western North America, A Review, *Geolog. Soc. of Amer. Mem.* **152**:1-30.
  17. Allmendinger, R.W., Hauge, T.A., Hauser, E.C., Potter, C.J., Klemperer, S.L., Nelson, K.D., Knuepfer, P., and Oliver, J. (1987) Overview of the COCORP 40 degree N Transect, Western United States: The Fabric of an Orogenic Belt, *Geolog. Soc. of Amer. Bull.* **98**:308-319.
  18. Burchfiel, B.C. and Davis, G.A. (1972) Structural Framework and Evolution of the Southern Part of the Cordilleran Orogen, Western United States, *Amer. J. of Sci.* **272**:97-118.
  19. Burchfiel, B.C. and Davis, G.A. (1975) Nature and Controls of the Cordilleran Orogenesis, Western United States - Extensions of an Earlier Synthesis, *Amer. J. of Sci.* **275-A**:275.
  20. Stewart, J.H. and Poole (1974) Lower Paleozoic and Uppermost Precambrian Cordilleran Miogeocline, Great Basin, Western United States, In Dickinson, W.R., ed., *Tectonics and Sedimentation*, Soc. of Econ. Paleontolog. and Mineralog. Spec. Pub. **22**:28-57.
  21. Stewart, J. H. (1972) Initial Deposits in the Cordilleran Geosyncline: Evidence of a Late Precambrian (< 850 m.y.) Continental Separation, *Geolog. Soc. of Amer. Bull.* **83**:1345-1360.

from Canada<sup>22</sup> through Idaho, western Montana, western Utah, eastern Nevada, and southern California into Mexico.<sup>23,24,25,26,27</sup> The central section in Nevada, from the Oregon and Idaho border on the north to the California border on the south, was the Cordilleran eugeosyncline.<sup>16</sup> West of the Cordillera were accreted terranes.<sup>17</sup>

The Antler Orogeny, thought to have occurred in Mississippian time<sup>28,29</sup> or late Devonian-early Mississippian<sup>30</sup>, extensively deformed rocks of the Basin and Range, causing eugeosynclinal rocks to be folded to the east over miogeosynclinal rocks along the Roberts Mountain thrust in Nevada. Minor orogenic pulses in the Basin and Range followed the Antler: the Sonoma Orogeny in the Permian (290 - 240 million years ago)<sup>31,32</sup> and the Nevadan Orogeny in the Jurassic (205 - 138 million years ago).<sup>30,33,34,35</sup> Marine and terrestrial deposits accumulated in the Colorado Plateau throughout the Paleozoic.<sup>5</sup>

- 
22. Canadian Geological Survey (1970) Geologic Map of Canada in Douglas, R.J.W., *Geology and Economic Minerals of Canada*, Canada Geologic Survey Economic Geology Report 1, Scale 1:5,000,000.
  23. Comite de la Carta Geologica de Mexico (1968) *Carte Geologica de la Republica Mexicana*, Scale 1:2,000,000.
  24. Lopez-Ramos, E. (1969) Marine Paleozoic Rocks of Mexico, *Amer. Assoc. of Petrol. Geol. Bull.* **53**:2399-2417.
  25. King, P.B. and Belkman, H.M. (1974) Geologic Map of the United States, U.S. Geological Survey Map, Scale 1:2,500,000.
  26. Gastil, R.G., Phillips, R.P., and Allison, E.C. (1975) Reconnaissance Geology of the State of Baja California, *Geol. Soc. of Amer. Mem.* **140**:170.
  27. Nicholas, R.L. and Rozendal, R.A. (1975) Subsurface Positive Elements within Ouachita Foldbelt in Texas and Their Relation to Paleozoic Cratonic Margin, *Amer. Assoc. of Petrol. Geol. Bull.* **59**:193-216.
  28. Roberts, R.J., Hotz, P.E., Gilluly, J., and Fergusson, H.G. (1958) Paleozoic Rocks of North-Central Nevada, *Amer. Assoc. of Petrol. Geol. Bull.* **42**:2813-2857.
  29. Speed, R.C. (1982) Evolution of the Sialic Margin in Central Western United States, in Watkins, J. and D. Drake eds., *Geology of Continental Margins*, *Amer. Assoc. of Petrol. Geol. Mem.* **34**:457-468.
  30. Bates, R.L. and Jackson, J.A. eds. (1984) *Dictionary of Geological Terms*, Anchor Press/Doubleday, NY, 3rd ed.
  31. Siberling, N.J. and Roberts, R.J. (1962) Pretertiary Stratigraphy and Structure of Northwestern Nevada, *Geol. Soc. of Amer. Spec. Paper* **72**:1-50.
  32. Speed, R.C. (1979) Collided Paleozoic Microplate in the Western United States, *J. of Geol.* **87**:279-292.
  33. Schweichert, R.A. and Cowan, D.S. (1975) Early Mesozoic Tectonic Evolution of the Western Sierra Nevada, California, *Geol. Soc. of Amer. Bull.* **86**:1329-1336.
  34. Schweichert, R.A. (1981) Tectonic Evolution of the Sierra Nevada Range, in Ernst, W.G. ed., *The Geotectonic Development of California*, Englewood Cliffs, New Jersey, Prentice-Hall, p87-131.
  35. Nelson, K.D., Zhu, T.F., Gibbs, A., Harris, R., Oliver, J.E., Kaufman, S., Brown, L.D., and Schweichert, A. (1985) COCORP Deep Seismic Reflection Profiling in the Northern Sierra Nevada, California, *Tectonics* **5**:321-333.



In Cretaceous through Eocene time (138 - 24 million years ago), the tectonics of the western margin of the United States were dominated by eastward plate subduction along an Andean-type continental margin.<sup>19,36,37,38</sup> Mountain building occurred as a result of subduction. The Sierra Nevada batholith was formed between 120 - 80 million years ago.<sup>39</sup> During the same time period, large plutons were intruded sparsely across Nevada into western Utah and also into southern Arizona and southern California.<sup>40,41,42</sup> Mountains were formed, trending northwest-southeast, during the Laramide Orogeny, which took place about 75 - 50 million years ago<sup>5</sup>, from British Columbia through Idaho, Montana, Wyoming, Colorado, and south into New Mexico. The Laramide Orogeny also produced elongate domical uplifts variable in trend throughout the Colorado Plateau.<sup>4</sup> Thrust faults resulting from the Sevier and Laramide Orogenies were oriented northwest-southeast throughout the northern Rocky Mountains and formed the division between the Basin and Range and both the Middle Rocky Mountains and the Colorado Plateau.<sup>14</sup>

The region presently called the Basin and Range Province underwent two periods of extension during Cenozoic time. The earlier extension oriented east-northeast<sup>43,44</sup>, and took place in mid-Oligocene (about 30 - 20 million years ago). This period was characterized by normal faulting, silicic volcanism, and local metamorphism.<sup>45,46,47</sup> Low angle normal faults were formed throughout the

- 
36. Hamilton, W. (1969) The Volcanic Central Andes - A Modern Model for the Cretaceous Batholiths and Tectonics of Western North America, *Oregon Dept. of Geolog. and Miner. Indus. Bull.* **65**:175-184.
  37. Coney, P.J. (1978) Mesozoic-Cenozoic Cordilleran Plate Tectonics, in Smith, R.B. and Eaton, G.P. Eds., *Cenozoic Tectonics and Regional Geophysics of the Western Cordillera*, *Geolog. Soc. of Amer. Mem.* **152**:33-50.
  38. Dickenson, W.R. and Snyder, W.S. (1978) Plate Tectonics of the Laramide Orogeny, In Mathews, V. Ed., *Laramide Folding Associated with Basement Block Faulting in the Western United States*, *Geolog. Soc. of Amer. Mem.* **151**:355-366.
  39. Chen, J.H. and Moore, J.G. (1982) Uranium-lead isotopic ages from the Sierra Nevada Batholith, California, *J. of Geophys. Res.* **87**:4761-4784.
  40. Hintze, L.F. (1973) Geologic History of Utah, *Brigham Young Univ. Geology Studies* **25**:181.
  41. Miller, C.F. and Bradfish, L.J. (1980) An Inner Cordilleran Belt of Muscovite-Bearing Plutons, *Geology* **8**:412-416.
  42. Stewart, J.H. (1980) Geology of Nevada, *Nevada Bur. of Mines and Geology Spec. Pub.* **4**:136.
  43. Zoback, M.L. and Thompson, G.A. (1978) Basin and Range Rifting in Northern Nevada: Clues from a Mid-Miocene Rift and Its Subsequent Offsets, *Geology* **6**:111-116.
  44. Zoback, M.L., Anderson, R.E., and Thompson, G.A. (1981) Cainozoic Evolution of the State of Stress and Style of Tectonism of the Basin and Range Province of the Western United States, *Roy. Soc. of London Philosop. Trans.* **A-300**:407-434.
  45. Davis, G.H. and Coney, P.J. (1979) Geologic Development of the Cordilleran Metamorphic Core Complexes, *Geology* **7**:120-124.
  46. Crittenden, M.D. Jr., Coney, P.J., and Davis, G.H., Eds. (1980) Cordilleran Metamorphic Core Complexes, *Geolog. Soc. of Amer. Mem.* **153**:490.
  47. Armstrong, R.L. (1982) Cordilleran Metamorphic Core Complexes - from Arizona to Southern Canada, *Annual Rev. of Earth and Planet. Sci.* **10**:129-154.

Basin and Range.<sup>48,49</sup> The later period of extension, oriented in an east-southeast direction, began about 10 million years ago.<sup>44</sup> This tectonic event created the typical Basin and Range features, which are characterized by evenly spaced blocks of mountains bounded by normal faults.<sup>17</sup>

Also during the late Cenozoic (17 million years to present) large volumes of basaltic lava erupted in the northwestern United States.<sup>50,51,52</sup> This volcanism extends north from along the northern border of the Basin and Range into Oregon, Idaho, and Washington.<sup>53</sup> Additional basaltic volcanism occurred along the southern and southwestern borders of the Colorado Plateau defining the Transition Zone between the Basin and Range and the Colorado Plateau.<sup>54</sup>

During the late Cenozoic, the Colorado Plateau has remained relatively undeformed. While the Basin and Range underwent two periods of extension (30 - 20 and 15 - 8 million years ago) the Colorado Plateau experienced uplift.<sup>5,44</sup> Two to five million years ago the Colorado Plateau was elevated again, reversing the direction of flow of the Little Colorado River. Before this period of uplift the Colorado River ran south. During the Pliocene, the Colorado River turned west and began to erode the Colorado Plateau, forming, among other features, the Grand Canyon.<sup>5</sup>

### 3. PAST SEISMIC STUDIES

Several previous seismic studies have taken place in the Colorado Plateau and Basin and Range. The line configurations of all of the past surveys discussed are found in Figure 2. In this section, surface wave analyses and seismic refraction and reflection surveys that took place in central and northwestern Arizona are reviewed. In addition, two three-component seismic refraction experiments that sampled an area between the northern Basin and Range and the northern Colorado Plateau are described.

Two refraction surveys in particular have been used extensively as a basis for other geophysical studies as well as for comparison of seismic survey results. One of these studies, centered at Tonto Forest Seismological Observatory, Arizona, was made up of an array of two 400 km lines.<sup>12</sup> One limb

- 
48. Armstrong, R.L. (1972) Low Angle (Denudation) Faults Hinterland of Sevier Orogenic Belt, Eastern Nevada and Western Utah, *Geolog. Soc. of Amer. Bull.* **83**:1729-1754.
  49. Proffett, J.M., Jr. (1977) Cenozoic Geology of the Yerrington District, Nevada, and Implications for the Nature and Origin of Basin and Range Faulting, *Geolog. Soc. of Amer. Bull.* **88**:247-266.
  50. McKee, E.H. (1971) Tertiary Igneous Chronology of the Great Basin of Western United States, Implications for Tectonic Models, *Geolog. Soc. of Amer. Bull.* **82**:3497-3502.
  51. Christiansen, R.L. and Lipman, P.W. (1972) Cenozoic Volcanism and Plate-Tectonic Evolution of the Western United States II, Late Cenozoic, *Roy. Soc. of London Philosop. Trans.* **271**:249-284.
  52. Noble, D.C. (1972) Some Observations on the Cenozoic Volcano-Tectonic Evolution of the Great Basin, Western United States, *Earth and Planet. Sci. Let.* **17**:142-150.
  53. McBirney, A.R., Sutter, J.F., Naslund, H.R., Sutton, K.G., and White, C.M. (1974) Episodic Volcanism in the Central Oregon Cascade Range, *Geology* **2**:585-589.
  54. Best, M.G. and Brimhall, W.H. (1974) Late Cenozoic Alkalic Basaltic Magmas in the Western Colorado Plateaus and the Basin and Range Transition Zone, USA and their Bearing on Mantle Dynamics, *Geolog. Soc. of Amer. Bull.* **85**:1677-1690.

of the array ran northwest-southeast following the boundary between the Colorado Plateau and the Transition Zone, and the other transected the southern Basin and Range and Colorado Plateau Provinces. Fourteen chemical explosions were recorded by an array of in-line, vertical-component stations, all located within the Transition Zone.

Models by Warren<sup>12</sup> are presented in Figure 5. A Pn velocity of 7.85 km/s was found for the entire survey area. For the Transition Zone, a crustal thickness of about 35 km is given. A crustal thickness of about 42 km is determined for the Colorado Plateau at the northeastern end of the northeast-southwest line, thinning to about 23 km in the southwest within the southern Basin and Range. The error given for the determination of the depth of the base of the crust was  $\pm 3$  km. An offset in the Moho of about 3 km was noted by Warren<sup>12</sup> beneath the Mogollon Rim, a prominent northwest trending topographic feature between the Basin and Range and the Colorado Plateau.

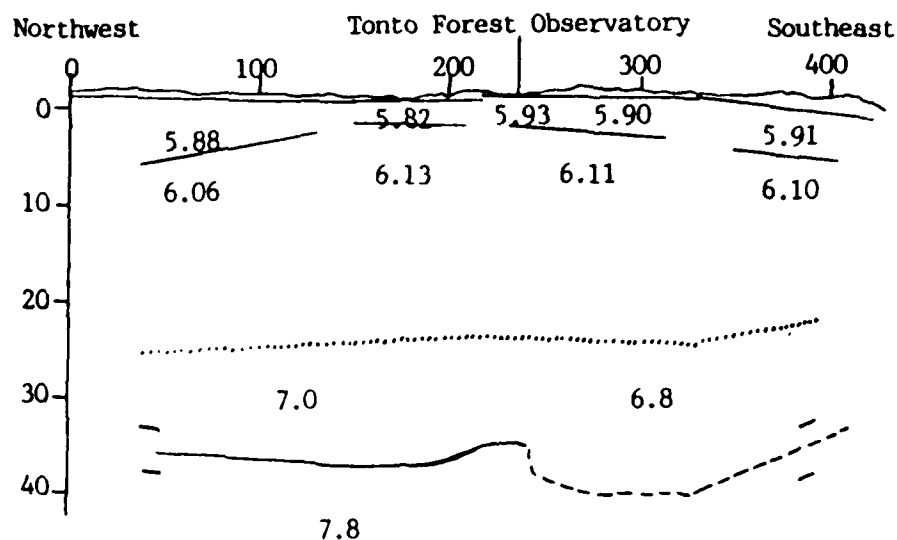
Shear arrivals were picked from the vertical-component seismograms. Although the shear arrivals were emergent, Warren<sup>12</sup> reported that the trend of shear first arrivals were correlated over several records and defined S-wave velocities for the layers corresponding to P-wave velocities of 5.8 km/s and 6.1 km/s (see Figure 5). Five shear velocities were calculated for each of these layers, ranging from 3.37 to 3.48 km/s for the 5.8 km/s compressional velocity layer and 3.63 to 3.82 km/s for the 6.1 km/s compressional velocity layer. Poisson's ratios were determined to be  $0.226 \pm 0.009$  and  $0.217 \pm 0.014$  for the 5.8 km/s and 6.1 km/s layers, respectively.

A survey that has often been used as a basis for other geophysical studies of the Colorado Plateau was done by Roller.<sup>8</sup> This was a 296 km reversed seismic refraction line from Hanksville, Utah, to Chinle, Arizona. Chemical explosions ranging in size from 2,000 to 10,000 pounds were set off in 200-foot boreholes. Four blasts were located at the north end of the line and three in the south. The model by Roller<sup>8</sup> shows 4 layers (Table 1c). A thin 2 km, 3.0 km/s layer is at the surface over a 24 km thick, 6.2 km/s upper crust layer. The Moho was reported to be about 38 km deep in the northwest. In the southeast, a depth to the Moho of 43 km was reported, in agreement with Warren.<sup>12</sup> A velocity of 7.8 km/s was indicated for the upper mantle of the Colorado Plateau. Located just above the Moho is a 6.8 km/s 16 - 18 km thick layer. Roller<sup>8</sup> indicated that the error associated with picking the first arrivals was  $\pm 0.1$  second and that the velocities were calculated within  $\pm 0.1$  km/s.

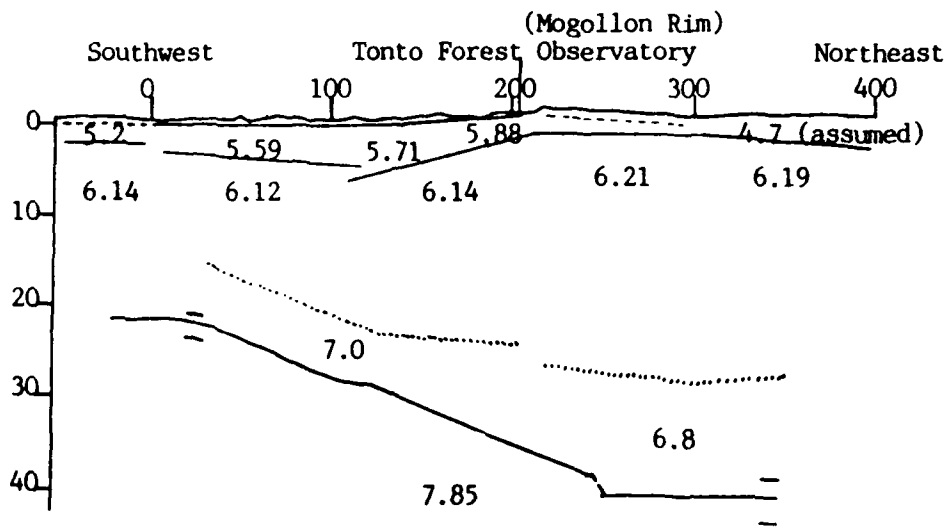
Another early seismic refraction survey in northwestern Arizona was set up between the Nevada Test Site and Kingman, Arizona, about 50 km northeast of Bagdad, Arizona.<sup>11</sup> Nuclear and chemical blasts, set off both above and below the surface in 1957 and 1958, provided the sources for the seismograms recorded along the 300 km line. The number of shots recorded or seismographs examined was not stated in the 1961 study. Stations were spaced irregularly, ranging from 10 km apart to 60 km apart. Some station sites included horizontal as well as vertical-component seismometers.

Diment and others<sup>11</sup> reported that the experiment resulted in data of poor quality, and they presented a simple layer-over-a-half space model. The authors (Diment and others, page 205)<sup>11</sup> state: "Beyond a distance of about 60 km from the explosions, the first arrivals are generally emergent and commonly difficult or impossible to determine with a precision of better than several tenths of a second."

Diment and others<sup>11</sup> go on to say that the horizontal-component data was even more emergent. Their crustal model (Table 2a) is a 28 km thick layer with a P velocity of 6.2 km/s over a layer of



(a)



(b)

Figure 5. Models presented by Warren.<sup>12</sup> (a) Model of the Transition Zone (b) Model of the region transecting the Basin and Range, Transition Zone, and the Colorado Plateau. The Mogollon Rim is in the vicinity of the Transition Zone - Colorado Plateau border. Dashed lines show less certain features. Dotted lines indicate the minimum depths that are permissible for the top of the intermediate layer. Velocities are in km/s.

Table 1. Models of the Colorado Plateau

(a) Keller and others<sup>7</sup>

| Thickness<br>(km) | P<br>(km/s) | S<br>(km/s) | $\sigma$ | Thickness<br>(km) | P<br>(km/s) | S<br>(km/s) | $\sigma$ |
|-------------------|-------------|-------------|----------|-------------------|-------------|-------------|----------|
| 1.73              | 3.40        | 2.00        | 0.25     | 1.40              | 3.40        | 1.90        | 0.25     |
| 6.70              | 6.00        | 3.50        | 0.24     | 14.10             | 5.90        | 3.50        | 0.24     |
| 6.30              | 5.50        | 2.90        | 0.31     | 9.90              | 6.40        | 3.20        | 0.33     |
| 10.00             | 6.50        | 3.50        | 0.29     | 7.40              | 4.00        | 0.28        |          |
|                   | 7.40        | 4.00        | 0.28     |                   |             |             |          |

(b) Brille and others<sup>6</sup>

| Thickness<br>(km) | P<br>(km/s) | S<br>(km/s) | $\sigma$ |
|-------------------|-------------|-------------|----------|
| 1.50              | 3.57        | 2.06        | 0.25     |
| 8.50              | 6.06        | 3.50        | 0.25     |
| 5.00              | 5.80        | 3.00        | 0.32     |
| 4.00              | 6.40        | 3.50        | 0.29     |
| 10.00             | 6.90        | 3.80        | 0.29     |
|                   | 7.60        | 4.25        | 0.28     |

(c) Roller<sup>8</sup>

| Thickness<br>(km) | P<br>(km/s) |
|-------------------|-------------|
| 2                 | 3.00        |
| 22 - 24           | 6.20        |
| 13 - 18           | 6.50        |
|                   | 7.80        |

Table 2. Models of the Colorado Plateau

(a) Diment and others<sup>11</sup>

| Thickness<br>(km) | P<br>(km/s) |
|-------------------|-------------|
| 28                | 6.20        |
|                   | 7.80        |

(b) Sinno and others<sup>1</sup>

| Thickness<br>(km) | P<br>(km/s) |
|-------------------|-------------|
| 14 - 16           | 6.05        |
| 10                | 6.40        |
|                   | 7.47        |

(c) McCarthy and others<sup>3</sup>

| Thickness<br>(km) | P<br>(km/s) |
|-------------------|-------------|
| 8                 | 6.00        |
| 9 - 10            | 5.90        |
| 3 - 5             | 6.80        |
| 4                 | 6.20        |
|                   | 7.80        |

(d) Langston and Helmberger<sup>10</sup>

| Thickness<br>(km) | P<br>(km/s) | S<br>(km/s) | $\sigma$ | Thickness<br>(km) | P<br>(km/s) | S<br>(km/s) | $\sigma$ |
|-------------------|-------------|-------------|----------|-------------------|-------------|-------------|----------|
| 1                 | 3.00        | 1.73        | 0.251    | 1                 | 3.00        | 1.73        | 0.251    |
| 1                 | 5.50        | 3.30        | 0.219    | 31                | 6.10        | 3.60        | 0.233    |
| 2                 | 5.90        | 3.40        | 0.251    | 7.90              | 4.60        | 0.244       |          |
| 25.5              | 6.10        | 3.60        | 0.233    |                   |             |             |          |
|                   | 7.90        | 4.60        | 0.244    |                   |             |             |          |

7.2 km/s. It is suggested by Diment and others<sup>11</sup> that a discontinuity deeper than 28 km may exist, indicating that 7.2 km/s may not be Pn but rather the velocity of a layer over the Moho discontinuity.

Surface wave analyses<sup>9,10</sup> were done along a path that crossed the PACE experiment shot line near Bagdad, Arizona. Bache and others<sup>9</sup> also examined a path transecting the Colorado Plateau and the southern Basin and Range (see Figure 2). The earlier analysis, done by Langston and Helmberger<sup>10</sup>, used data collected between the Nevada Test Site and Luke Air Force Base in line with Tucson, Arizona. Eight Caltech portable broadband seismograph trailers were deployed along the approximately 450 km line. The seismic source for the Langston and Helmberger<sup>10</sup> study was a single underground nuclear blast. Additional data collected from the Nevada Test Site to the Tucson World Wide Standard Seismographic Network (WWSSN) station were analyzed as a control for determining the structure of the top half of the crust. Shear-wave velocities for the Basin and Range were calculated from the inversion of Rayleigh wave data. Two southern Basin and Range models developed by Langston and Helmberger<sup>10</sup> are presented in Table 2d. A crustal thickness of 29.5 - 32 km is indicated with upper crustal P and S velocities of 6.1 km/s and 3.6 km/s, respectively. Pn and Sn velocities of 7.9 km/s and 4.6 km/s are given. An error of  $\pm 0.1$  km/s was noted for compressional velocities. Poisson's ratios of 0.233 and 0.244 were calculated for the upper and lower crust, respectively.

Bache and others<sup>9</sup> examined data from the Nevada Test Site-Phoenix path, which passes through the southern Basin and Range, as well as the Nevada Test Site-Albuquerque path, which transects the southern Basin and Range and the Colorado Plateau (Figure 2). Their purpose was to test an improved method for determining crustal velocity models through the use of synthetic seismograms. Because of this, models from previous works were used as constraints on the inversion. A Pn of 7.9 km/s was chosen as a typical velocity value for the Basin and Range Province from previous studies.<sup>10,11,12</sup> In the upper crust, a Poisson's ratio of 0.23 was assumed, taken from Langston and Helmberger.<sup>10</sup> For the Nevada Test Site-Albuquerque path, Bache and others<sup>9</sup> used an average Moho depth of 42 km, based on Prodehl, Topozada and Sanford, Keller and others, and Wickens and Pec.<sup>55,56,57,58</sup> From the analysis of Bache and others (1978) shear velocities for the upper mantle were found to be 4.4 km/s for the Nevada Test Site-Phoenix path and 4.3 km/s for the Nevada Test Site-Albuquerque path. These shear velocities resulted in Poisson's ratios of  $0.27 \pm 0.01$  for the Nevada Test Site-Phoenix path and  $0.29 \pm 0.01$  km/s for the Nevada Test Site-Albuquerque path.

A reversed seismic refraction survey was done along a 290 km line from Parker to Globe, Arizona, almost parallel to the northwest-southeast line of Warren<sup>12</sup>, and crossing the PACE shot

- 
55. Prodehl, C. (1970) Seismic Refraction Study of Crustal Structure in the Western United States, *Geolog. Soc. of Amer. Bull.* **81**(9):2629-2646.
  56. Topozada, T. and Sanford, A.R. (1976) Crustal Structure in Central New Mexico Interpreted from the Gasbuggy Explosion, *Bull. of the Seismolog. Soc. of Amer.* **66**(3):877-886.
  57. Keller, G.R., Smith, R.B., Bralle, L.W., Heaney, R., and Shurbet, D.H. (1976) Upper Crustal Structure of the Eastern Basin and Range, Northern Colorado Plateau, and Middle Rocky Mountains from Rayleigh Wave Dispersion, *Bull. of the Seismolog. Soc. of Amer.* **66**(3):869-876.
  58. Wickens, A.J. and Pec, K. (1968) A Crust-Mantle Profile from Mould Bay, Canada, to Tucson, Arizona, *Bull. of the Seismolog. Soc. of Amer.* **58**(6):1821-1831.

line.<sup>1</sup> Mine shots in Globe at the southeast end of the line and an explosion at Miser's Bluff in the northeast were the sources for the experiment. Station spacing averaged 6 km. The first layer of the three-layer crustal model presented (Table 2b) was about 14 - 16 km thick with a velocity of  $6.05 \pm 0.05$  km/s. A second layer was 8 to 10 km thick and had a velocity of  $6.4 \pm 0.15$  km/s. The Moho was found to be about 23-25 km deep, about the same as the depth Warren<sup>12</sup> calculated for the line where it crossed the Parker to Globe line. A Pn of  $7.67 \pm 0.05$  km/s was found for the southern Basin and Range, a value intermediate between 7.85 km/s from Warren<sup>12</sup> and 7.2 km/s from Diment et al.<sup>11</sup>

A seismic refraction study that took place in the area between the northern Basin and Range and the Colorado Plateau<sup>7</sup> and one that took place in the region between the northern Basin and Range and Middle Rocky Mountain Province<sup>6</sup> are included in this review because three-component data were collected and shear-wave velocities presented in those two studies. The sources for the two surveys were copper mine explosions at Bingham Copper Mine in Utah. One 245 km line running almost due south from the mine had 66 stations about 3.5 km apart, on average. The other line, made up of 98 sites averaging about the same station spacing, extended northeast 340 km from the source. Two models presented by Keller and others<sup>7</sup> for the north-south line transecting the northern Basin and Range and the Colorado Plateau are in Table 1a. Table 1b shows a part of the crustal model of Braille and others<sup>6</sup>, the portion that describes the crustal velocity structure of the northern Basin and Range. A thin crust of about 25 km was presented in the area south of the mine. To the northeast a Moho depth of 28 km was reported. Low upper mantle P and S velocities of  $7.4 \pm 0.1$  km/s and 4.0 km/s for the north-south line and  $7.6 \pm 0.1$  km/s and 4.25 km/s for the southwest-northeast oriented line were determined. Keller and others<sup>7</sup> suggested that the low Pn of 7.4 km/s could be an apparent velocity if a dipping discontinuity exists. One of the models in Table 1a and the model in Table 1b include a low velocity layer in the crust. Keller and others<sup>7</sup> point to a low velocity layer reported in the eastern side of the northern Basin and Range<sup>59,60</sup> in support of their model with such a layer. High Poisson's ratios of 0.29 and 0.28 are reported for the two deeper layers in both of the studies.

Recently, a COCORP seismic reflection profile<sup>13</sup> was carried out in the vicinity of the survey analyzed in this study. Data was collected along a line extending about 200 km southwest from Bagdad, Arizona toward the California border and along another line extending out from Camp Wood about 60 km to the northeast (Figure 2). Reflection data was not collected directly under the entire AFGL line, which was located between the two towns. Figure 4 shows the Arizona reflection profile, the resulting crustal structure of Hauser and others<sup>13</sup>, and the relationship between the array location and the towns of Bagdad and Camp Wood. Three features are emphasized in this figure: (1) A shallow reflective surface appears to take on the anticlinal configuration centered about 115 - 125 km southwest of Bagdad and is reported<sup>13</sup> to be the Buckskin-Rawhide metamorphic core complex. (2) The upper 15 km of the Transition Zone crust is characterized by many reflective interfaces, termed the Bagdad reflection sequence.<sup>13</sup> This sequence extends about 80 km to the northeast from Highway 93,

---

59. Mueller, S. and Landisman, M. (1971) An Example of the Unified Method of Interpretation for Crustal Seismic Data, *Geophys. J. Roy. Astron. Soc.* **23**:365-371.

60. Mueller, G. and Mueller, S. (1972) A Crustal Low-Velocity Zone in Utah, *Geolog. Soc. Amer. Abstr. Programs* **4**:204

which is indicated in Figure 4. (3) Offsets in the Moho up to 3 km are suggested, with the depth to the Moho discontinuity at about 9 - 10 s two-way travel time (27 - 30 km) in the Basin and Range, 10 - 10.5 s (30 - 32 km) in the area of Bagdad, and about 12 s (about 36 km) at Camp Wood (see Figure 4).

Two USGS PACE seismic refraction surveys have been done to date.<sup>2,3</sup> The first survey took place in 1985 in the Whipple Mountains on the southern California-Arizona border within the southern Basin and Range<sup>2</sup> (Figure 2). Two perpendicular, reversed profiles recorded 30 shots from 20 shot points. Station spacing was 0.5 km on the northeast trending line and 1.0 km on the northwest trending line. The model presented for the northeast line as a result of 2-dimensional raytracing<sup>2</sup> includes two low velocity layers, one in the upper crust and one in the lower crust (Table 2c). An upper mantle velocity of 7.8 km/s is reported for both lines with a depth to Moho of 26 - 27 km. McCarthy and others<sup>2</sup> do not present a model for the northwest trending line. However, they state that no low-velocity zones are present and that a model would include little vertical velocity variation. The upper crust in this direction shows a more uniform 6.0 km/s down to the upper mantle boundary.

The second PACE seismic refraction experiment took place in northwestern Arizona from Quartzite to Camp Wood, Arizona (Figure 2).<sup>3</sup> Two deployments, each made up of 240 vertical-component seismometers set 0.75 km apart, received 27 shots from 19 shot points. Preliminary results<sup>2</sup> revealed a depth to the Moho of 30 km on the southwest end of the line and 32 km at the northeast of the line. A prominent mid-crustal layer about 22 km is suggested. Apparent Pn velocities of 7.7 km/s to the southwest and 7.9 km/s to the northeast were reported. Strong reflections in the Bagdad region support the existence of the Bagdad reflection sequence.<sup>13</sup> McCarthy and others<sup>3</sup> note that the seismic records from the southwest show strong reflections, in contrast to weak reflections in the records from the northeast.

Beghoul and Barazangi<sup>61</sup> analyzed P-wave data collected from multiple paths through the Colorado Plateau. Using a two-station method, hundreds of earthquakes from an ISC data set were analyzed for the Pn velocity, with the result of  $8.1 \pm 0.09$  km/s being calculated. In this method, events were chosen that were located at distances where: (1) Pn was seen as a first arrival ( $2^\circ - 16^\circ$ ), (2) the path was across the Colorado Plateau, and (3) the path was in or very near the azimuth of the two-station pair. Only the difference in travel times between the two stations was used in the velocity calculations. The velocity reported by Beghoul and Barazangi<sup>61</sup> is higher than the Pn velocities of 7.85 reported by Warren<sup>12</sup>,  $7.8 \pm 0.1$  km/s reported by Roller<sup>8</sup>, and  $7.4 \pm 0.1$  km/s reported by Keller and others.<sup>7</sup> Hauser and Lundy<sup>14</sup> interpreted COCORP seismic reflection data collected in the southwestern part of the Colorado Plateau as having a reflective interface at 16 s two-way travel time. This implied a Moho depth of about 50 km, which is deeper than the previously published central Colorado Plateau depth of 40 - 43 km.<sup>8</sup> It is stated<sup>14</sup> that an unreasonably low mean crustal velocity of 5.0 km/s would have to be assumed to get a depth of 40 km at 16 seconds. A mean velocity of 6.2 km/s was used to yield a 50 km depth. The authors reported the mantle as being generally unreflective with no apparent boundary or surface in the reflection data at the expected time of 13 seconds for a 40 - 43 km depth.

---

61. Beghoul, M.N. and Barazangi, M. (1988) Relatively High Pn Velocity Beneath the Colorado Plateau Constrains Uplift Models, *EOS Trans.* **69**(16):496.



Because the Moho depths of Hauser and Lundy<sup>14</sup> did not coincide with those of Roller<sup>8</sup> and Warren<sup>12</sup>, Hauser and Lundy<sup>14</sup> reinterpreted the older refraction data assuming the Pn velocity of  $8.1 \pm 0.09$  km/s that had been calculated by Beghoul and Barazangi.<sup>61</sup> The original model of Warren<sup>12</sup> was modified in two ways: (1) The step in the Moho in the original model (Figure 5) was increased from 3 - 4 km to 10 km. (2) The Pn velocity to the northeast of the rim was increased to 8.1 km/s. The Pn velocity used for the Basin and Range section of the modified model was 7.85 km/s, the same as the original model.<sup>12</sup> When the alternative model was raytraced, Hauser and Lundy<sup>14</sup> reported that they were able to closely match (the error is not stated) theoretical travel times to the observed travel times published by Warren.<sup>12</sup> Hauser and Lundy<sup>14</sup> pointed out that the depth to Moho published by Warren<sup>12</sup> was calculated by the delay time method and based on the assumed Pn velocity of 7.85 km/s. When Hauser and Lundy<sup>14</sup> recalculated the Colorado Plateau crustal thickness using a Pn of 8.1 km/s, they found a depth of 50 km.

Hauser and Lundy<sup>14</sup> reevaluated the seismograms of Roller.<sup>8</sup> In this analysis, Hauser and Lundy<sup>14</sup> pointed out that the data<sup>8</sup> displayed weak Pn arrivals and that the PmP reflections from the Moho were extremely difficult to pick out and correlate from trace to trace. Hauser and Lundy<sup>14</sup> developed a plane-layer model with a 50 km thick crust with a 6.5 km/s velocity and with a Pn velocity of 8.1 km/s. Using this plane-layered model, the travel time curve for the Pn fits the data published by Roller<sup>8</sup> to within  $\pm 0.1$  second.

To summarize, the central and southeastern edges of the Colorado Plateau have been characterized by Roller<sup>8</sup> and Warren<sup>12</sup> as having similar velocity structures. Upper crustal and lower crustal velocities are reported in both studies to be 6.2 and 6.8 km/s respectively while Pn velocities are  $7.8 \pm 0.1$  km/s<sup>8</sup> and 7.8 km/s.<sup>12</sup> Beghoul and Barazangi<sup>61</sup> report an average Pn velocity for the Colorado Plateau of  $8.1 \pm 0.09$  km/s, in disagreement with Roller<sup>8</sup> and Warren.<sup>12</sup> Hauser and Lundy<sup>14</sup> describe a crustal thickness of about 50 km which is thicker than the  $42 \pm 3$  km of Warren<sup>12</sup> and Roller<sup>8</sup> based on a  $7.8 \pm 0.1$  km/s Pn velocity. Hauser and Lundy<sup>14</sup>, however, show that these data<sup>8,12</sup> could be reinterpreted to result in a crustal thickness in the Colorado Plateau of about 50 km and an upper mantle velocity of 8.1 km/s.

The crustal and upper mantle velocities of the southern Basin and Range do not appear to be distinctly different from those of the Transition Zone between the southern Basin and Range and the southern Colorado Plateau. Upper crustal velocities are reported to be about 6.1 km/s.<sup>1,10,12</sup> Pn velocities described are 7.67 km/s,<sup>1</sup> 7.85 km/s,<sup>12</sup> 7.8 km/s,<sup>2,11</sup> and 7.7 - 7.9 km/s.<sup>3</sup> The thickness of the crust was found to be 28.5 - 31 km along the Nevada Test Site-Phoenix path.<sup>9,10,11</sup> The thickness along the Transition Zone was found to be  $35 \pm 3$  km, thinning to  $23 \pm 3$  km in the southern Basin and Range.<sup>2,3,12</sup> Sinno and others<sup>1</sup> found the crustal thickness to be about the same as that of Warren<sup>12</sup> in the area where lines of the two investigations crossed.

Shear upper mantle velocities reported for the southern Basin and Range and Transition Zone are 4.6 km/s for the Nevada Test Site-Phoenix path.<sup>10</sup> Langston and Helmberger<sup>10</sup> present a crustal shear velocity of 3.6 km/s which compares to the lower of the 3.63 - 3.82 km/s range of velocities presented by Warren<sup>12</sup> for a path roughly parallel to the Nevada Test Site-Phoenix path.

The structures described by Keller and others<sup>7</sup> and Braille and others<sup>6</sup> in the Transition Zone north of the Colorado Plateau are quite different from those in central and northwestern Arizona. In addition to a 5 or 6 km low velocity zone in this northern region, a thin 24.7 km crust is described by

Keller and others.<sup>7</sup> Poisson's ratios in the deep layers (3 - 5) of the northern Basin and Range-Colorado Plateau transition zone range from 0.28 - 0.31 while those in the southern Basin and Range<sup>10</sup> are slightly below 0.25.

#### 4 EXPERIMENTAL DETAILS

Three sets of USGS PACE shots set off on the night of 4 - 5 June 1987 were used as sources for this study. Shot locations are shown in Figure 3 and are listed in Table 3. Although the AFGL recording line was located entirely within the Transition Zone, the shots were fired within both the Colorado Plateau and the Basin and Range. Thirteen 40-meter borehole shots were fired in line with the stations, including one within the station array between BD08 and BD09. The shot array stretched from 180.6 km to the southwest to 131.8 km to the northeast of the AFGL line. This resulted in the recording of arrivals from as far away as about 215 km from the southwest and almost 170 km to the northeast. The explosive used for the source was a slurry of ammonium nitrate and diesel fuel. Shot sizes ranged from 500 lb (230 kg) to 6000 lb (2700 kg).

The 27 stations comprising the AFGL line were deployed at approximately 1.5 km intervals, forming a line 35.4 km long along the road from Bagdad to Camp Wood. (Figure 3). Station BD01 is the farthest site to the southwest, with station numbers increasing toward the northeast. Station locations are given in Table 4. Three-component seismometers were installed at each site. The seismometers were buried in shallow holes to insure good coupling in the ground. North-south horizontal-components were lined up with magnetic North (declination 14.5 degrees East) and east-west components were set perpendicular to them.

DCS-302 three-channel digital recorders with automatic gain ranging were used to record the data for this study. The data were recorded on cassette tapes at a rate of 100 samples per second, per channel. Two types of seismometers were deployed. HS10-1B one-second period instruments were used at seven stations. The remaining stations were equipped with S-6000 triaxial seismometers with a natural period of 0.5 s (Table 5).

The internal clocks of the recorders were synchronized with the GOES satellite clock before and after the night of shooting to gauge the drift of the individual clocks. As an additional measure to achieve accurate timing, recorders at stations BD13 through BD27 were equipped with antennas and recorded a WWVB signal on tape simultaneously with the recorded data. Seven stations were manually turned on and off while the remaining were triggered by alarm clocks attached to the recorders.

Because the WWVB signal was not clear for station BD17 and the time synchronization notes for this station are missing from the field logs, the BD17 traces were not included in this analysis. The recorder for station BD08 was initially set 3 seconds off. This error was taken into account when processing the data from the first two shot windows. Since it was neglected in the processing of the third shot window, the 3 seconds show up in the time corrections for the last three shots shown in Table 6c. The internal clock failed on the recorder used at station BD19, and the WWVB time trace was employed to determine the calibration of the internal clock to absolute time. Since the internal clock was drifting relative to the WWVB time, the time corrections applied to succeeding shot windows varied considerably for station BD19. Time corrections for each shot are found in Tables 6a, b, and c.

Table 3. Source Information from the Pacific-Arizona Crustal Experiment

| Shot ID # | Shot Point | Year | Day | Hour | Minute | Second  | Latitude (Degrees N) | Longitude (Degrees W) | Elevation (Meters) | Size (lbs) |
|-----------|------------|------|-----|------|--------|---------|----------------------|-----------------------|--------------------|------------|
| SH14      | 27         | 1987 | 155 | 5    | 0      | 0.0100  | 34.3113              | -113.5716             | 380                | 1500       |
| SH15      | 20         | 1987 | 155 | 5    | 2      | 0.0050  | 33.4860              | -114.5967             | 36                 | 5000       |
| SH16      | 31         | 1987 | 155 | 5    | 4      | 0.0100  | 34.8075              | -112.8953             | 1742               | 2000       |
| SH17      | 34         | 1987 | 155 | 5    | 6      | 0.0120  | 35.6536              | -111.8595             | 1932               | 6000       |
| SH18      | 29         | 1987 | 155 | 5    | 8      | 0.0080  | 34.5395              | -113.2260             | 1069               | 1000       |
| SH19      | 26         | 1987 | 155 | 7    | 30     | 0.0100  | 34.2716              | -113.6327             | 420                | 2000       |
| SH20      | 21         | 1987 | 155 | 7    | 31     | 59.8810 | 33.6829              | -114.2785             | 283                | 4000       |
| SH21      | 30         | 1987 | 155 | 7    | 34     | 0.0100  | 34.6737              | -113.0916             | 1490               | 1000       |
| SH22      | 33         | 1987 | 155 | 7    | 36     | 0.0120  | 35.3926              | -112.2360             | 1850               | 4000       |
| SH23      | 36         | 1987 | 155 | 7    | 38     | 0.0070  | 34.5118              | -113.2596             | 929                | 500        |
| SH24*     | 7          | 1987 | 155 | 10   | 0      | 0.0100  | 34.6901              | -113.9399             | 813                | 2000       |
| SH25      | 23         | 1987 | 155 | 10   | 1      | 59.9550 | 33.9588              | -113.9966             | 265                | 3000       |
| SH26      | 32         | 1987 | 155 | 10   | 4      | 0.0100  | 35.0824              | -112.6225             | 1490               | 3000       |
| SH27      | 28         | 1987 | 155 | 10   | 6      | 0.0070  | 34.4648              | -113.3458             | 887                | 1000       |

\* Shot point 7 (SH24) was offset and, therefore, not included in this analysis.

Table 4. Station Locations

| Station ID # | Latitude<br>(Degrees N) | Longitude<br>(Degrees W) | Elevation<br>(Meters) | Corresponding<br>USGS Station # |
|--------------|-------------------------|--------------------------|-----------------------|---------------------------------|
| BD01         | 34.5911                 | -113.1606                | 1201                  | USGS 303                        |
| BD03         | 34.6121                 | -113.1394                | 1317                  | USGS 307                        |
| BD04         | 34.6216                 | -113.1280                | 1326                  | USGS 309                        |
| BD05         | 34.6302                 | -113.1157                | 1350                  | USGS 311                        |
| BD06         | 34.6388                 | -113.1031                | 1289                  | USGS 313                        |
| BD07         | 34.6516                 | -113.0956                | 1344                  | USGS 315                        |
| BD08         | 34.6699                 | -113.0954                | 1527                  | USGS 317                        |
| BD09         | 34.6794                 | -113.0908                | 1561                  | USGS 319                        |
| BD10         | 34.6848                 | -113.0723                | 1576                  | USGS 321A                       |
| BD11         | 34.6893                 | -113.0586                | 1590                  | USGS 323A                       |
| BD13         | 34.7137                 | -113.0495                | 1676                  | USGS 327A                       |
| BD14         | 34.7276                 | -113.0414                | 1675                  | NO USGS #                       |
| BD15         | 34.7403                 | -113.0337                | 1700                  | NO USGS #                       |
| BD16         | 34.7548                 | -113.0249                | 1701                  | USGS 333                        |
| BD17         | 34.7567                 | -113.0039                | 1737                  | USGS 335                        |
| BD18         | 34.7611                 | -112.9853                | 1792                  | USGS 337                        |
| BD19         | 34.7691                 | -112.9717                | 1768                  | USGS 339                        |
| BD20         | 34.7843                 | -112.9717                | 1780                  | NO USGS #                       |
| BD21         | 34.7893                 | -112.9604                | 1790                  | NO USGS #                       |
| BD22         | 34.7928                 | -112.9474                | 1820                  | NO USGS #                       |
| BD23         | 34.7944                 | -112.9331                | 1804                  | NO USGS #                       |
| BD24         | 34.7946                 | -112.9211                | 1792                  | USGS 346                        |
| BD25         | 34.7999                 | -112.9053                | 1823                  | USGS 348                        |
| BD26         | 34.8001                 | -112.8856                | 1756                  | NO USGS #                       |
| BD27         | 34.8072                 | -112.8759                | 1731                  | NO USGS #                       |

Table 5. Instrument Constants

RECORDERS

Terra Technology digital cassette recorder

Model: DCS 302

Channels: 3

Sample Rate: 100 samples/s/channel

Anti-alias Filter 3 dB point: 30 Hz

Digitizer: 5 Volts 0-4095

Automatic Gain Ranging: Gains:

1. Stations BD1, BD3 - BD10: 10, 250, 500, 1000
2. Stations BD13, BD14, BD17 - BD27: 100, 2500, 5000, 10000
3. Stations BD2, BD11: 1, 25, 50, 100

SEISMOMETERS

Hall-Sears single axis seismometer

Model: HS-10-1B used for stations BD1, BD4, BD6, BD8, BD10, and BD11

Natural frequency: 1 Hz

Damping ratio: 1

Sensitivity: 1150.0 volts/m/s

Sprengnether triaxial seismometer

Model: S-6000 used for stations BD3, BD5, BD7, BD9, BD13 - BD27

Natural frequency: 2 Hz

Damping ratio: 1

Sensitivity: 200.0 volts/m/s

Table 6a. Time Corrections in Seconds

## First Shot Window

| Station ID # | SHOT 14 | SHOT 15 | SHOT 16 | SHOT 17 | SHOT 18 |
|--------------|---------|---------|---------|---------|---------|
| BD01         | -0.0338 | -0.0338 | -0.0338 | -0.0338 | -0.0338 |
| BD03         | -0.1129 | -0.1129 | -0.1129 | -0.1129 | -0.1129 |
| BD04         | -0.0623 | -0.0623 | -0.0623 | -0.0623 | -0.0623 |
| BD05         | +0.1809 | +0.1809 | +0.1809 | +0.1809 | +0.1809 |
| BD06         | +0.0629 | +0.0629 | +0.0629 | +0.0629 | +0.0629 |
| BD07         | +0.0326 | +0.0326 | +0.0326 | +0.0326 | +0.0326 |
| BD08         | +0.0540 | +0.0540 | +0.0540 | +0.0540 | +0.0540 |
| BD09         | -0.0845 | -0.0845 | -0.0845 | -0.0845 | -0.0845 |
| BD10         | +0.0409 | +0.0409 | +0.0409 | +0.0409 | +0.0409 |
| BD11         | +0.1600 | +0.1600 | +0.1600 | +0.1600 | +0.1600 |
| BD13         | -0.0394 | -0.0394 | -0.0394 | -0.0394 | -0.0394 |
| BD14         | -0.0668 | -0.0668 | -0.0668 | -0.0668 | -0.0668 |
| BD17         | ---     | ---     | ---     | ---     | ---     |
| BD18         | -0.0668 | -0.0668 | -0.0668 | -0.0668 | -0.0668 |
| BD19         | +0.0732 | +0.0732 | +0.0732 | +0.0732 | +0.0732 |
| BD20         | +0.0532 | +0.0532 | +0.0532 | +0.0532 | +0.0532 |
| BD21         | -0.0068 | -0.0068 | -0.0168 | -0.0168 | -0.0168 |
| BD22         | +0.0332 | +0.0332 | +0.0332 | +0.0332 | +0.0332 |
| BD23         | +0.0432 | +0.0432 | +0.0432 | +0.0432 | +0.0432 |
| BD24         | +0.1590 | +0.1590 | +0.1590 | +0.1590 | +0.1590 |
| BD25         | -0.0668 | -0.0668 | -0.0668 | -0.0668 | -0.0668 |
| BD26         | +0.0932 | +0.0932 | +0.0932 | +0.0932 | +0.0932 |
| BD27         | +0.4732 | +0.4732 | +0.4732 | +0.4732 | +0.4732 |

Table 6b. Time Corrections in Seconds

## Second Shot Window

| Station ID # | SHOT 19 | SHOT 20 | SHOT 21 | SHOT 22 | SHOT 23 |
|--------------|---------|---------|---------|---------|---------|
| BD01         | -0.0428 | -0.0428 | -0.0428 | -0.0428 | -0.0428 |
| BD03         | -0.1459 | -0.1459 | -0.1459 | -0.1459 | -0.1459 |
| BD04         | -0.0833 | -0.0833 | -0.0833 | -0.0833 | -0.0833 |
| BD05         | +0.2319 | +0.2319 | +0.2319 | +0.2319 | +0.2319 |
| BD06         | +0.0854 | +0.0854 | +0.0854 | +0.0854 | +0.0854 |
| BD07         | +0.0446 | +0.0446 | +0.0446 | +0.0446 | +0.0446 |
| BD08         | +0.0735 | +0.0735 | +0.0735 | +0.0735 | +0.0735 |
| BD09         | -0.1220 | -0.1220 | -0.1220 | -0.1220 | -0.1220 |
| BD10         | +0.0590 | +0.0590 | +0.0590 | +0.0590 | +0.0590 |
| BD11         | +0.2303 | +0.2303 | +0.2303 | +0.2303 | +0.2303 |
| BD13         | -0.0646 | -0.0646 | -0.0646 | -0.0646 | -0.0646 |
| BD14         | -0.1068 | -0.1068 | -0.1068 | -0.1068 | -0.1068 |
| BD17         | ---     | ---     | ---     | ---     | ---     |
| BD18         | -0.0968 | -0.0968 | -0.0968 | -0.0968 | -0.0968 |
| BD19         | -0.4286 | -0.4286 | -0.4286 | -0.4286 | -0.4286 |
| BD20         | +0.0632 | +0.0632 | +0.0632 | +0.0632 | +0.0632 |
| BD21         | -0.0168 | -0.0168 | -0.0168 | -0.0168 | -0.0168 |
| BD22         | +0.0432 | +0.0432 | +0.0332 | +0.0432 | +0.0432 |
| BD23         | +0.0532 | +0.0532 | +0.0532 | +0.0532 | +0.0532 |
| BD24         | +0.2010 | +0.2010 | +0.2010 | +0.2010 | +0.2010 |
| BD25         | -0.0888 | -0.0888 | -0.0888 | -0.0888 | -0.0888 |
| BD26         | +0.1132 | +0.1132 | +0.1132 | +0.1132 | +0.1132 |
| BD27         | +0.5714 | +0.5714 | +0.5714 | +0.5714 | +0.5714 |

Table 6c. Time Corrections in Seconds

## Third Shot Window

| Station ID # | SHOT 25 | SHOT 26 | SHOT 27 |
|--------------|---------|---------|---------|
| BD01         | -0.0518 | -0.0518 | -0.0518 |
| BD03         | -0.1789 | -0.1789 | -0.1789 |
| BD04         | -0.1043 | -0.1043 | -0.1043 |
| BD05         | +0.2829 | +0.2829 | +0.2829 |
| BD06         | +0.1079 | +0.1079 | +0.1079 |
| BD07         | +0.0566 | +0.0566 | +0.0566 |
| BD08         | +3.0930 | +3.0930 | +3.0930 |
| BD09         | -0.1595 | -0.1595 | -0.1595 |
| BD10         | +0.0769 | +0.0769 | +0.0769 |
| BD11         | +0.3008 | +0.3008 | +0.3008 |
| BD13         | -0.0754 | -0.0754 | -0.0754 |
| BD14         | -0.1396 | -0.1396 | -0.1396 |
| BD17         | ---     | ---     | ---     |
| BD18         | -0.1278 | -0.1278 | -0.1278 |
| BD19         | +0.0479 | +0.0479 | +0.0479 |
| BD20         | +0.0732 | +0.0732 | +0.0732 |
| BD21         | -0.0206 | -0.0206 | -0.0206 |
| BD22         | +0.0627 | +0.0627 | +0.0627 |
| BD23         | +0.0632 | +0.0632 | +0.0632 |
| BD24         | +0.2433 | +0.2433 | +0.2433 |
| BD25         | -0.0968 | -0.0968 | -0.0968 |
| BD26         | +0.1232 | +0.1232 | +0.1332 |
| BD27         | +0.6695 | +0.6695 | +0.6695 |



The experiment resulted in numerous good quality records despite the recorder failures at station BD01 and BD17 for most of the shots. Stations BD02 and BD12 were never installed due to faulty instruments. The recorders, which automatically gain range down when a large signal is detected, do not automatically gain range back up afterwards. This feature created a problem when a shot was fired very close to the stations. The recorders automatically gain ranged down, truncating the record for that shot, and remained down for any subsequent shot recorded before the instrument could be manually reset. This affected the amplitude resolution on some of the records. The AFGL records examined do not include data from stations BD15 and BD16. The data from these two stations were collected on Boston College and MIT instruments (DR-200) and have not yet been processed.

## 5. INTERPRETATION

The purpose of this study was to develop compressional and shear velocity structures for the southern Basin and Range, the Colorado Plateau, and the Transition Zone between them from the AFGL data collected in northwestern Arizona. Raytracing was the principal technique used in the analysis. The initial crustal compressional velocity structures used to begin modeling the AFGL data were developed by the USGS from USGS PACE data recorded at their stations located near the AFGL stations<sup>3</sup> (see Figure 6). This initial USGS model was tested against the AFGL compressional wave data. A few alterations, which are explained later in this section, had to be made to this initial model in order to fit the AFGL P-wave travel times. After the development of new P velocity crustal structures for the three geologic regions of this study, S-velocity structures were developed and the Poisson's ratios calculated for the crust in each region.

Following a description of the AFGL seismograms, this section is divided into two segments. In the first segment, the USGS model of crustal compressional velocity structures is presented. The compressional velocity crustal structures from this study for the southern Basin and Range, the Colorado Plateau, and the Transition Zone are then described. Evidence supporting the alterations and additions to the USGS model in the development of the AFGL model is given. The second segment of this section describes the shear velocity structures and Poisson's ratios developed in this study.

Throughout the following discussion, a standard notation will be used to represent particular P and S phases.  $P_g$  and  $S_g$  will be used to describe refractions from the thick upper crustal layer (layer 2) which lies below a thin surficial layer of sediments and sedimentary rock.  $P_n$ ,  $S_n$  and  $P_mP$ , and  $S_mS$  describe refractions and reflections from the Moho. Refractions and reflections from the boundary between layer 2 and 3 are represented by  $P_3$ ,  $S_3$ , and  $P_3P$  and  $S_3S$ , and for the boundary between layer 3 and 4 they are  $P_4$ ,  $S_4$ ,  $P_4P$ , and  $S_4S$ .

Before the arrival times picked from the AFGL records are interpreted, some differences in the characteristics of the seismograms between those from the southwest and from those from the northeast should be pointed out. Composite record sections encompassing data from a given direction (northeast or southwest) are shown in Figure 7 and Figure 8. Figure 7 includes seismograms from both the vertical and north-south horizontal-components from shot point 26 (SH19), shot point 23 (SH25), shot point 21 (SH20), and shot point 20 (SH15). Together, these shots, all located southwest of the stations, provide a record section for distances of 54 to 217 km. Figure 8 includes records from the

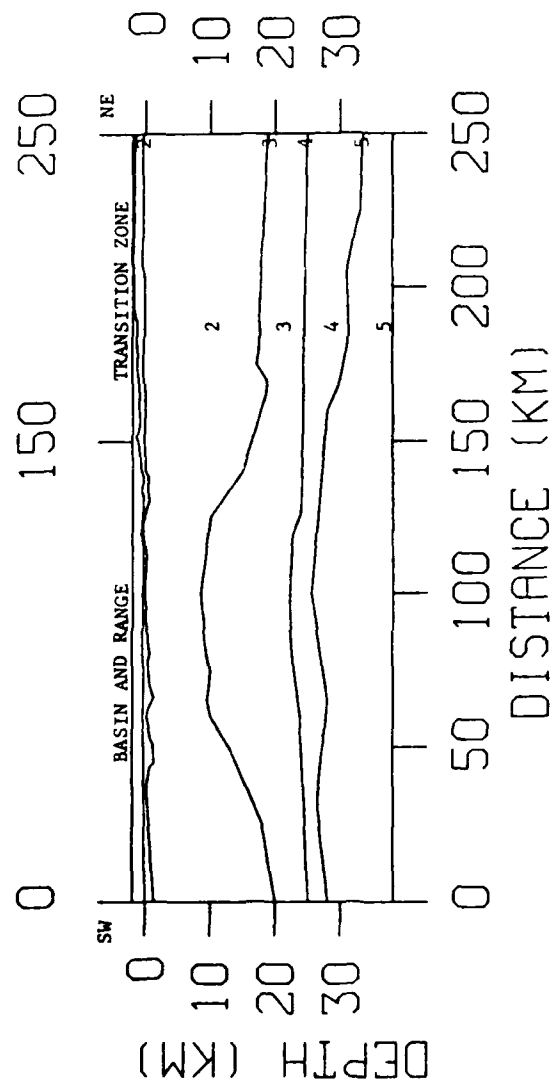
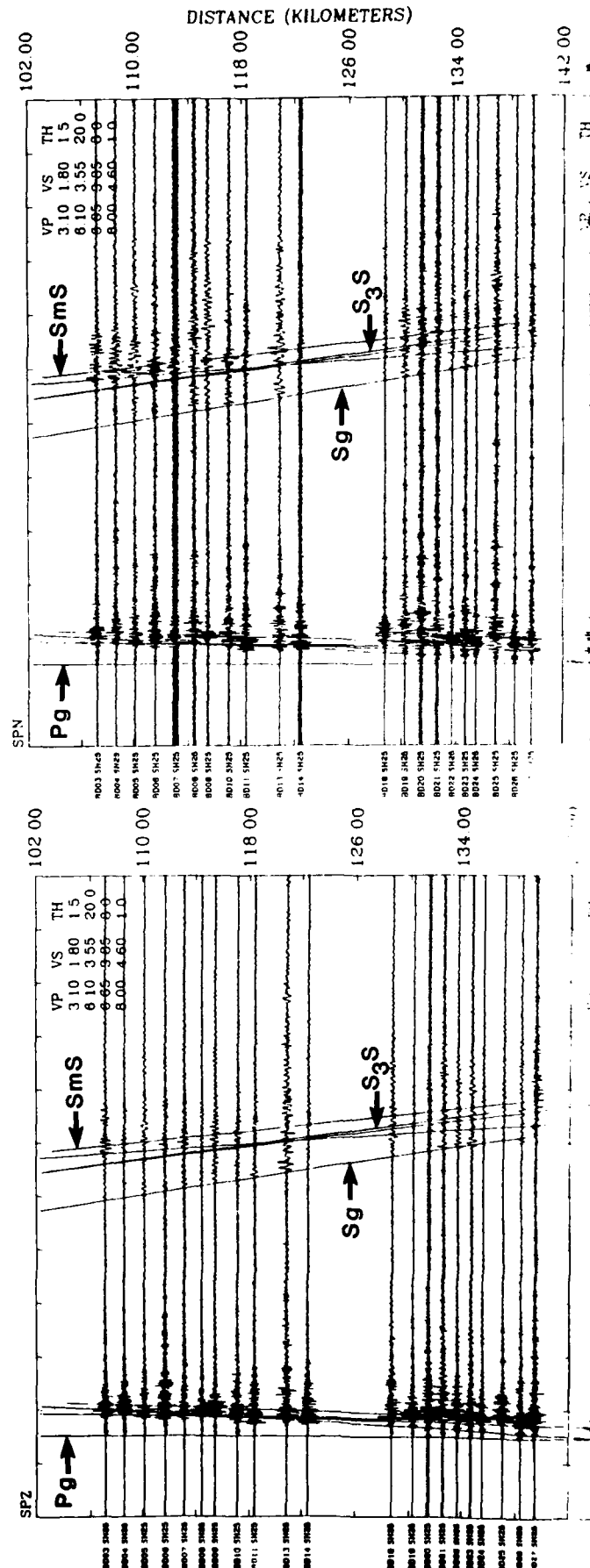
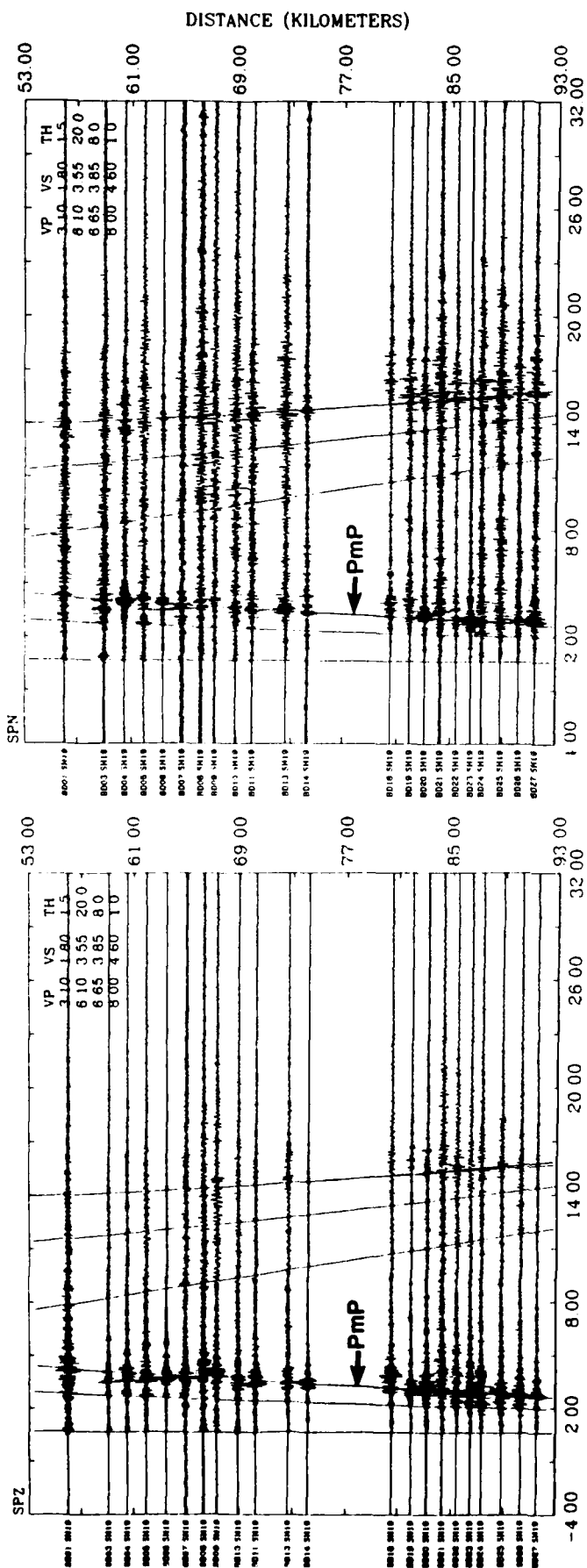


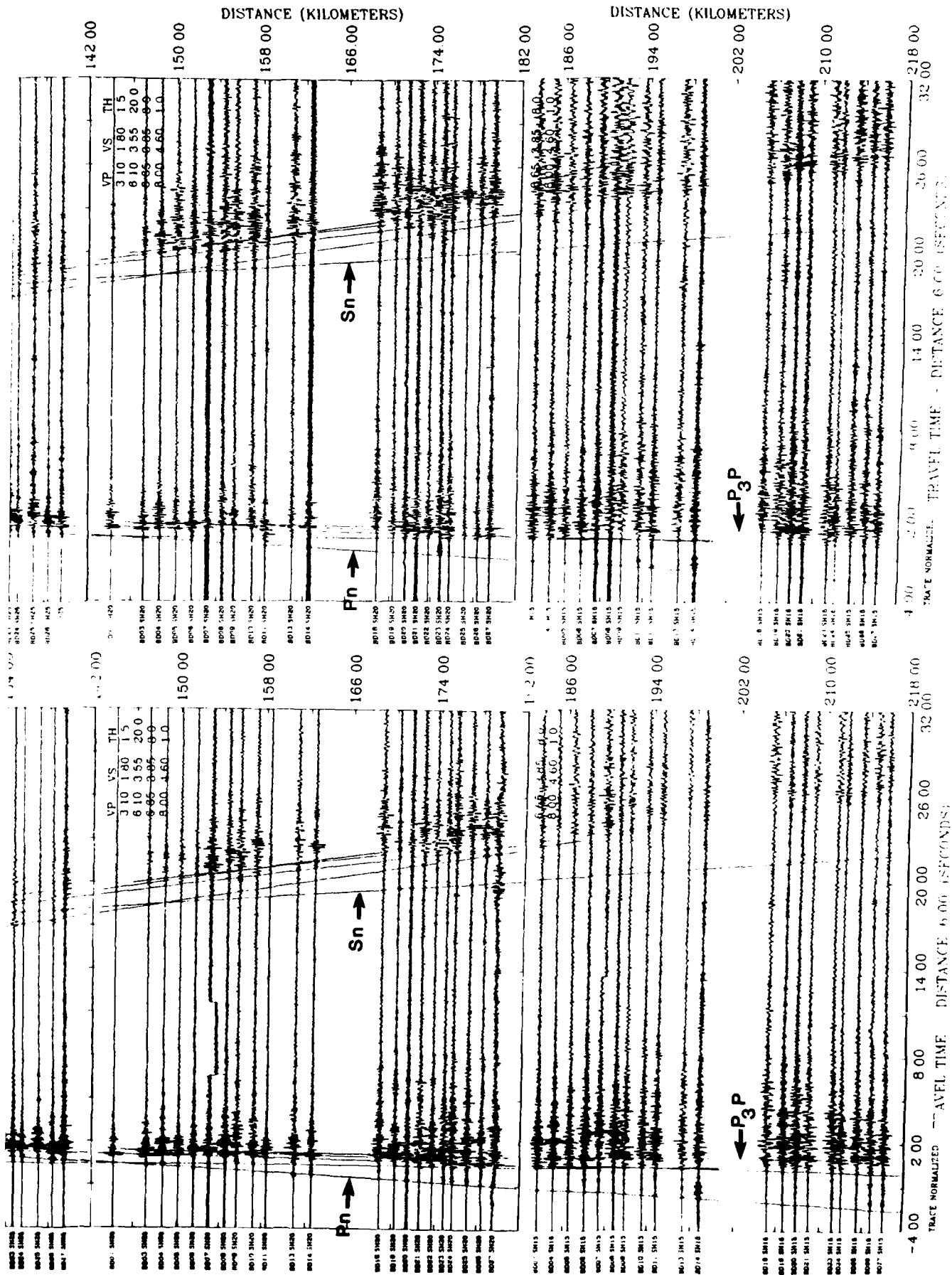
Figure 6. Initial Model Used for Raytracing.<sup>3</sup> The datum is sea level. Shot point 20 (SH15) is located at 0 on the model. Velocity gradients can be found in Table 7a.

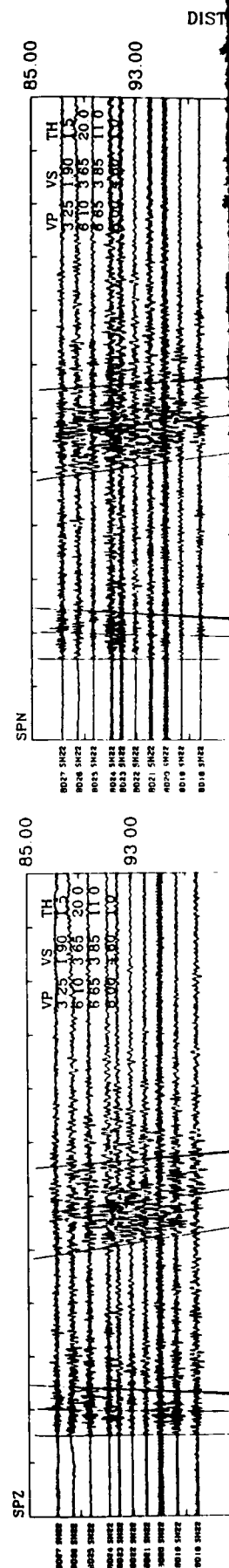
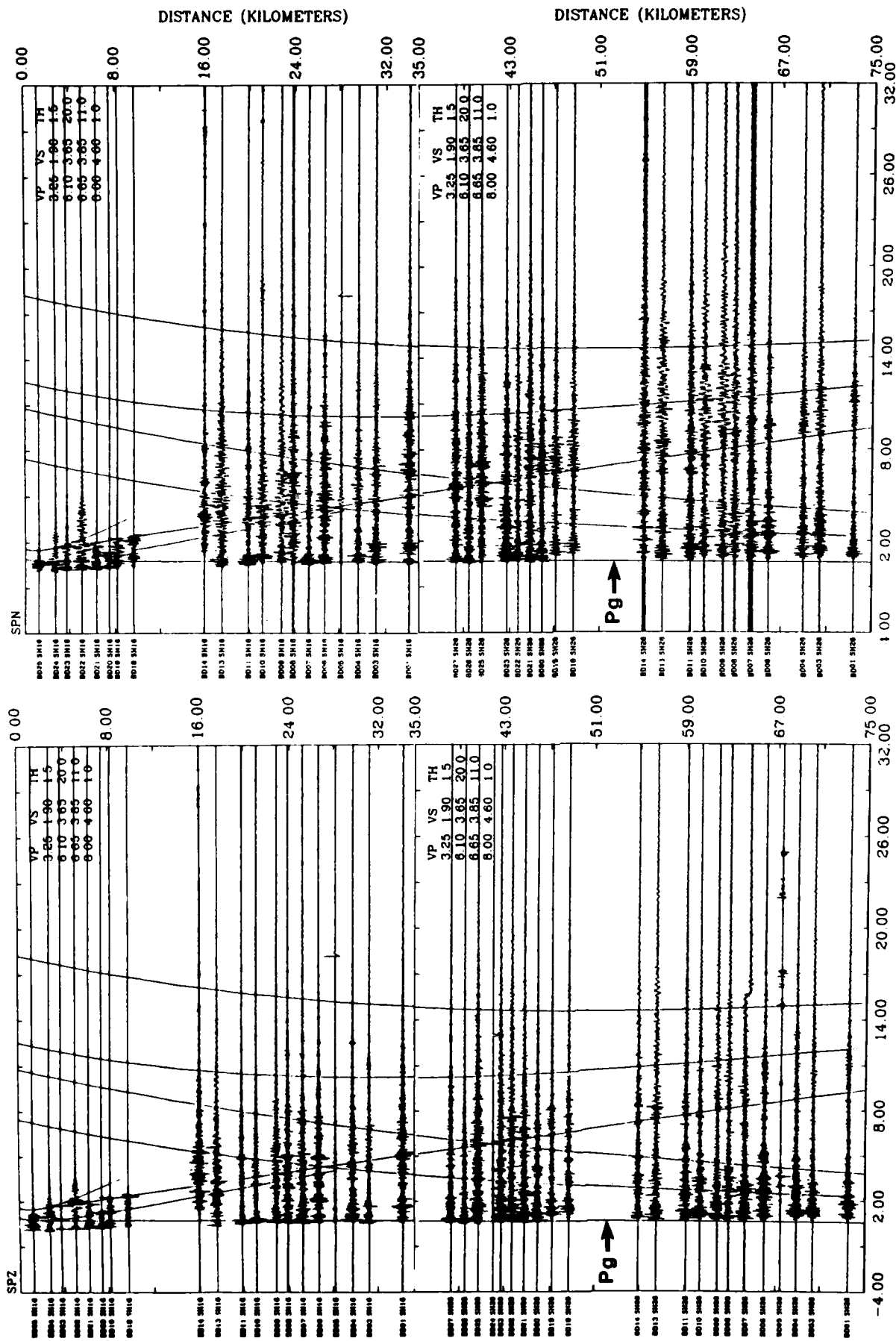
The figures on the following pages are composite record sections of vertical and north-south horizontal-component data collected from shots to the northeast and from shots to the southwest. The record sections are trace-normalized, relative amplitude plots. The superimposed travel time curve was generated by a plane-layer, constant layer velocity travel time program.

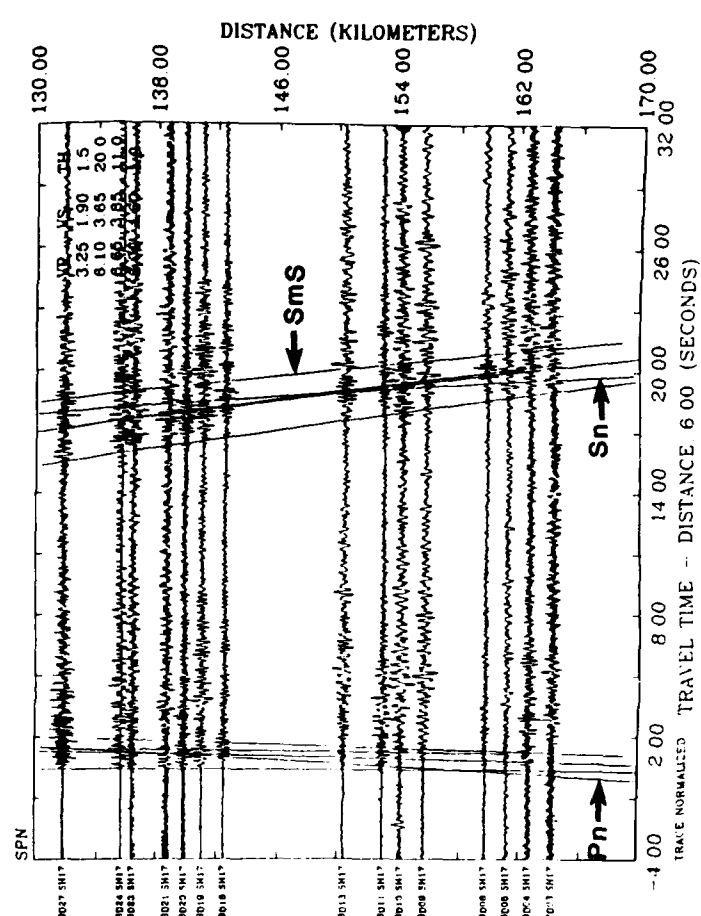
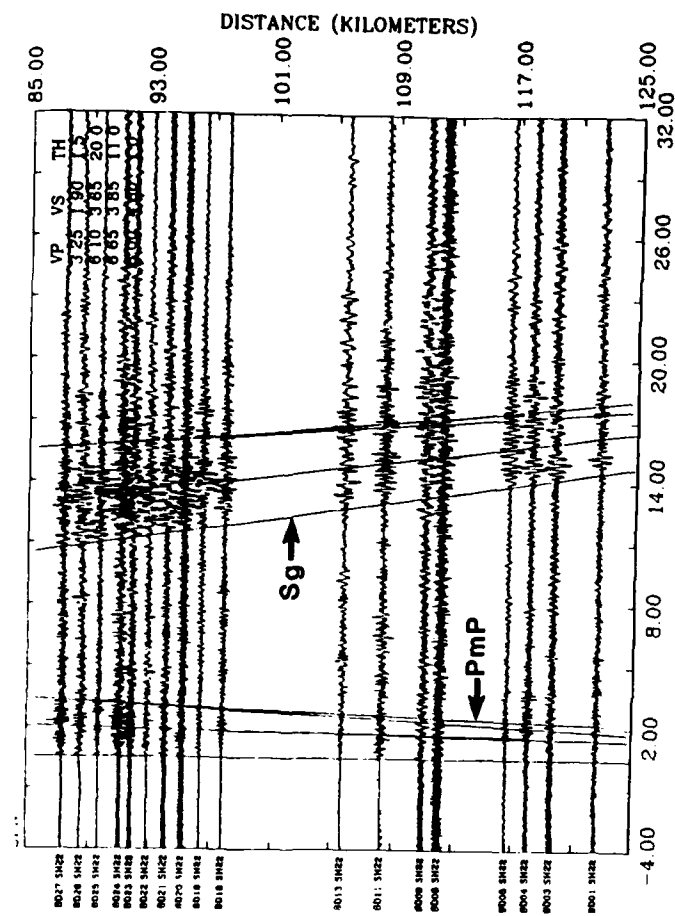
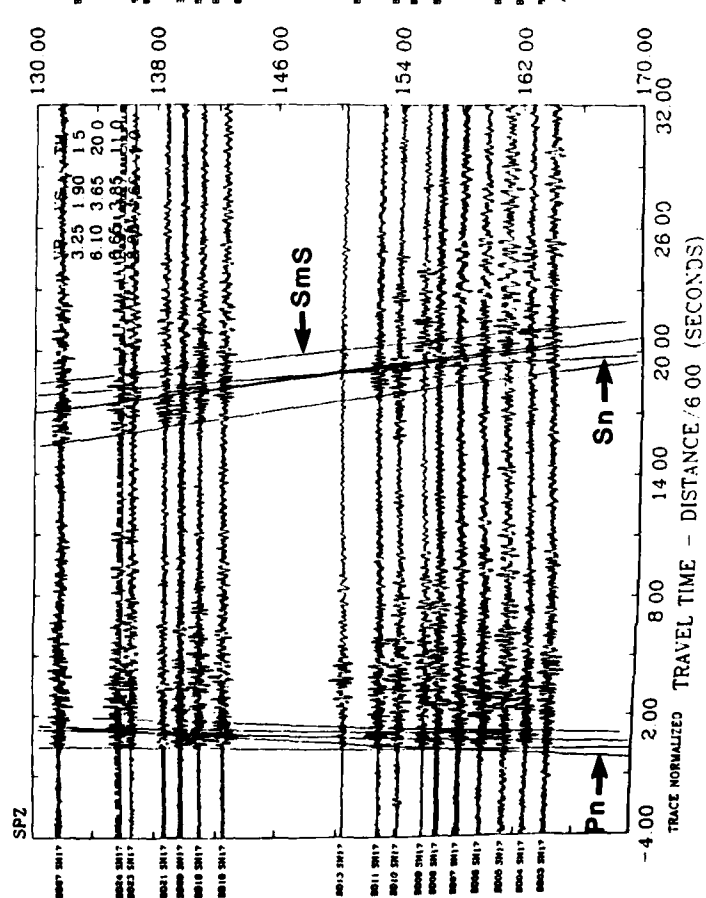
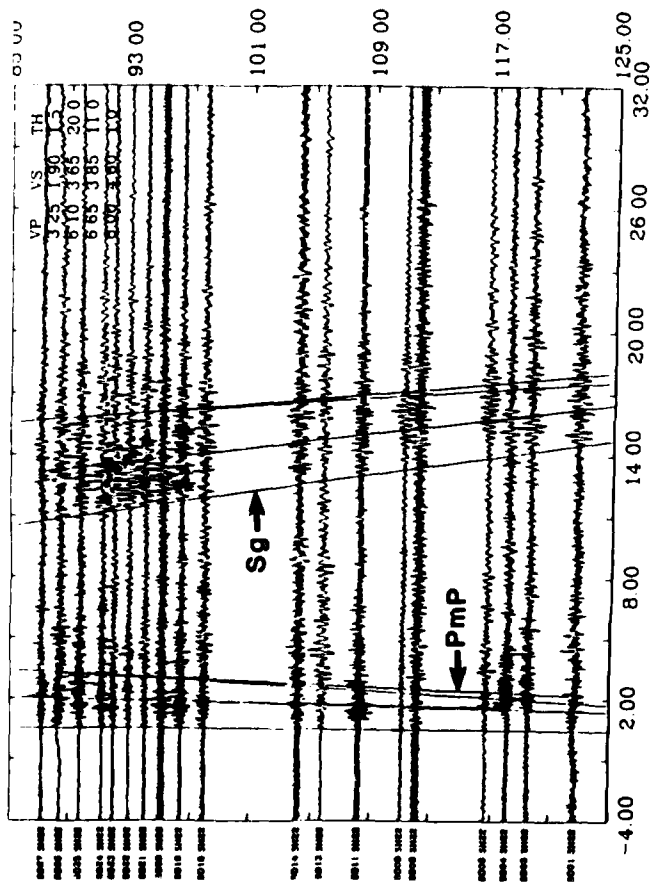
Figure 7. Composite Seismic Records from Shots Southwest of the Stations with a Superimposed Travel Time Curve. Shown are Shot Point 26 (SH19), Shot Point 23 (SH25), Shot Point 21 (SH20), and Shot Point 20 (SH15). The travel time curve is based on a plane-layer model for the Basin and Range. The vertical-component record section is on the bottom of the page and the horizontal-component record section is on the top. (Page 29)

Figure 8. Composite Seismic Records from Shots Northeast of the Stations with a Superimposed Travel Time Curve. Shown are Shot Point 31 (SH16), Shot Point 32 (SH26), Shot Point 33 (SH22), and Shot Point 34 (SH17). The travel time curve is based on a plane-layer model comparable to the AFGL model for the Colorado Plateau-Transition Zone area. The vertical-component record section is on the bottom of the page and the horizontal-component record section is on the top. (Page 30)









vertical and north-south horizontal component of shots from the northeast: shot point 31 (SH16), shot point 32 (SH26), shot point 33 (SH22), shot point 34 (SH17). The distance range included from the northeast is 0 to 165 km.

The most obvious difference between these two record sections is that there are two strong reflective phases (labeled  $P_3P$ ,  $S_3S$  and  $PmP$ ,  $SmS$ ) in Figure 7 from the southwest while strong coherent reflections from the northeast in Figure 8 are distinctly lacking. Because the records in Figure 8 are lacking in large amplitude reflections, the relative amplitude plots from the northeast emphasize the  $P_g$  and  $S_g$  phases.

Another feature to observe in Figures 7 and 8 is that of the  $P_n$  phase, the reflection from the Moho discontinuity. In Figure 7,  $P_n$  becomes the first arrival in the region 140 - 150 km from the shots to the southwest. The  $P_n$  phase cannot be seen distinctly as the first arrival up to the distance of 165 km for the shots from the northeast in Figure 8, suggesting that the Moho discontinuity is at a greater depth beneath the Colorado Plateau than beneath the Basin and Range.

Arrival times of P and S phases were picked from the unfiltered relative amplitude plots. The records are of excellent quality, allowing P-wave first arrivals to be picked within about  $\pm 0.04$  seconds from shots from either the northeast or southwest. Later compressional arrivals from shots to the southwest were generally picked to within  $\pm 0.1$  second. Neither P nor S reflections could confidently be determined from northeast shots beyond about 75 km. Shear second arrivals could generally be picked to within  $\pm 0.3$  seconds.

The principal method used for the analysis of the seismograms for the crustal structure was two-dimensional raytracing.<sup>62</sup> In this analysis, theoretical travel times for rays propagating through a given crustal P or S velocity structure are calculated. The calculated travel times are then compared with observed travel times. Adjustments in the crustal structure and/or velocity structure are made, if necessary, in an attempt to get calculated theoretical travel times to match observed travel times. In the model, the velocities at the top and bottom of each layer are used to parameterize the velocity gradient within that layer. Lateral variations in velocities are allowed in order to represent a heterogeneous material. In this study, theoretical travel times were generally matched to within  $\pm 0.1$  second of observed travel times.

Plane-layer modeling was employed to efficiently investigate possible modifications of the USGS crustal velocity structure. Large changes in structure and upper mantle P-wave velocities could be examined more quickly with a constant velocity, plane-layer model than with the raytracing program. This method was also used in an attempt to identify some of the P and S phases observed to ensure that particular rays were directed along expected paths while raytracing.

## 5.1 Crustal Compressional Velocity Structure

Because this study intended to focus on the shear structure of the study area, the analysis began with a USGS developed crustal compressional velocity structure model.<sup>3</sup> (Figure 6 and Table 7a). Shot

---

62. Luetgert, J.H. (1988) Users Manual for RAY84/R83PLT Interactive Two-Dimensional Raytracing/Synthetic Seismogram Package, U.S. Geological Survey Open File Report No. 88-238, 52p.



point 20 (SH15) is at 0 distance on this starting model. The Basin and Range part of the profile is from 0 to about 150 km. From 150 - 250 km, the profile represents the velocity structure of the Transition Zone.

There are no lateral variations in the velocities of the USGS model listed in Table 7a. Therefore, no distinction is made in this model between the velocity structures of the Basin and Range and the Transition Zone. The crustal structure of the initial USGS model, however, indicate some differences between the two regions. Layer 2 in the Transition Zone appears to be 17 - 19 km thick. Layer 4 in this region thickens to the northeast resulting in the depth to the Moho in the Transition Zone of 28 - 33 km. In contrast, layer 2 in the southern Basin and Range is about 18 km thick in the southwest near the California border and thins to a minimum of 8 - 9 km about 100 km to the northeast before thickening again near the Transition Zone. Layer 3 in the Basin and Range, which is thin (4 - 5 km) at the edges of this province, thickens to about 15 km around 100 km northeast of shot point 20 (SH15). The southern Basin and Range Moho is approximately 26.5 to 28 km deep.

The crustal model that resulted from this study will be referred to as the AFGL model. It is largely an extension of the a USGS model, with one major alteration in the Basin and Range upper crustal structure. Figure 9 shows the raytracing diagram; Figure 10 is a cartoon of the structures with velocities and Poisson's ratios. The AFGL model is a 5 layer, 350 km long profile. Like the USGS model, 0 - 150 km of the profile represents the southern Basin and Range and the Transition Zone falls between about 150 - 250 km. The AFGL model has been extended to include a part of the Colorado Plateau between 250 - 350 km. The PACE shot point 34 (SH17), which was the shot furthest to the northeast, is located near 350 km. Velocities presented are resolved to  $\pm 0.1$  km/s and the error associated with the depths of the layers is  $\pm 1$  km.

The AFGL Basin and Range model (Figure 9) has a thin, irregular surficial layer with a compressional velocity range of about 2.66 - 3.5 km/s. The upper crustal layer (layer 2) is about 18 - 20 km thick and has a velocity ranging from 6.01 - 6.22 km/s. Layers 3 and 4, each about 3 - 5 km thick, have velocities of 6.28 - 6.45 km/s and 6.53 - 6.63 km/s, respectively. The depth to the Moho was determined to be 26.5 - 28 km, and the upper mantle velocity for the southern Basin and Range is 8.0 km/s.

The major alteration in the USGS Basin and Range model was the flattening out of the interface between layers 2 and 3. In the USGS model interface 3 (Figure 6) was arched to be compatible with the structure observed in the COCORP records<sup>13</sup> labeled as mylonitic layering beneath the Buckskin-Rawhide detachment in Figure 4. Theoretical travel times of refractions and reflections from the USGS crustal structure were about 0.5 s earlier than those on the high amplitude traces found on the AFGL records for shot point 20 (SH15). Shot point 20 was the shot farthest to the southwest. Small variations in the velocities and thicknesses of layers 2, 3, and 4 within the Basin and Range did not fit the arrivals within the  $\pm 0.1$  second error found for the arrivals from the other shots from the southwest. Figure 11 shows raytracing results from shot point 20 before interface 3 was flattened. Figure 12 shows raytracing results from the same shot point after interface 3 was flattened. Because reflected arrivals from interface 3 and refracted arrivals from layer 2 match the observed travel times near 1 s reduced travel time, the USGS P-wave structure was modified to the AFGL model.

Table 7. Velocity Information in Kilometers Per Second

(a) Initial USGS Raytracing Model Compressional Velocities

| Layer | Velocity (km/s) |
|-------|-----------------|
| 1     | 2.50 - 3.50     |
| 2     | 6.00 - 6.20     |
| 3     | 6.30 - 6.40     |
| 4     | 6.55 - 6.60     |
| 5     | 8.00 - 8.10     |

(b) AFGL Raytracing Model Compressional and Shear Velocities

| Layer | Basin and Range |             | Transition Zone |             | Colorado Plateau* |             |
|-------|-----------------|-------------|-----------------|-------------|-------------------|-------------|
|       | P               | S           | P               | S           | P                 | S           |
| 1     | 2.66 - 3.50     | 1.52 - 2.03 | 2.71 - 3.60     | 1.56 - 2.10 | 2.68 - 3.80       | 1.57 - 2.18 |
| 2     | 6.01 - 6.22     | 3.44 - 3.59 | 6.06 - 6.31     | 3.52 - 3.69 | 6.06 - 6.22       | 3.64 - 3.74 |
| 3     | 6.28 - 6.45     | 3.71 - 3.75 | 6.37 - 6.55     | 3.76 - 3.81 | 6.51 - 6.59       | 3.77 - 3.80 |
| 4     | 6.53 - 6.63     | 3.80 - 3.83 | 6.58 - 6.68     | 3.83 - 3.85 | 6.68 - 6.75       | 3.86 - 3.90 |
| 5     | 8.00 - 8.10     | 4.62 - 4.68 | 7.95 - 8.02     | 4.59 - 4.65 | 7.96 - 8.05       | 4.60 - 4.65 |

(c) Average Velocities and Poisson's Ratios for the AFGL Model

| Layer | Basin and Range |      |          | Transition Zone |      |          | Colorado Plateau* |      |          |
|-------|-----------------|------|----------|-----------------|------|----------|-------------------|------|----------|
|       | P               | S    | $\sigma$ | P               | S    | $\sigma$ | P                 | S    | $\sigma$ |
| 1     | 3.08            | 1.78 | 0.249    | 3.16            | 1.83 | 0.248    | 3.24              | 1.88 | 0.246    |
| 2     | 6.12            | 3.52 | 0.253    | 6.19            | 3.61 | 0.242    | 6.14              | 3.69 | 0.217    |
| 3     | 6.37            | 3.73 | 0.239    | 6.46            | 3.79 | 0.238    | 6.55              | 3.79 | 0.248    |
| 4     | 6.58            | 3.82 | 0.246    | 6.63            | 3.84 | 0.248    | 6.72              | 3.88 | 0.250    |
| 5     | 8.00            | 4.62 | 0.250    | 7.95            | 4.59 | 0.250    | 7.96              | 4.60 | 0.249    |

\* Velocities in layers 3 - 5 of the Colorado Plateau are not well defined due to poor resolution in the records from the northeast (See ray paths in Figure 9).

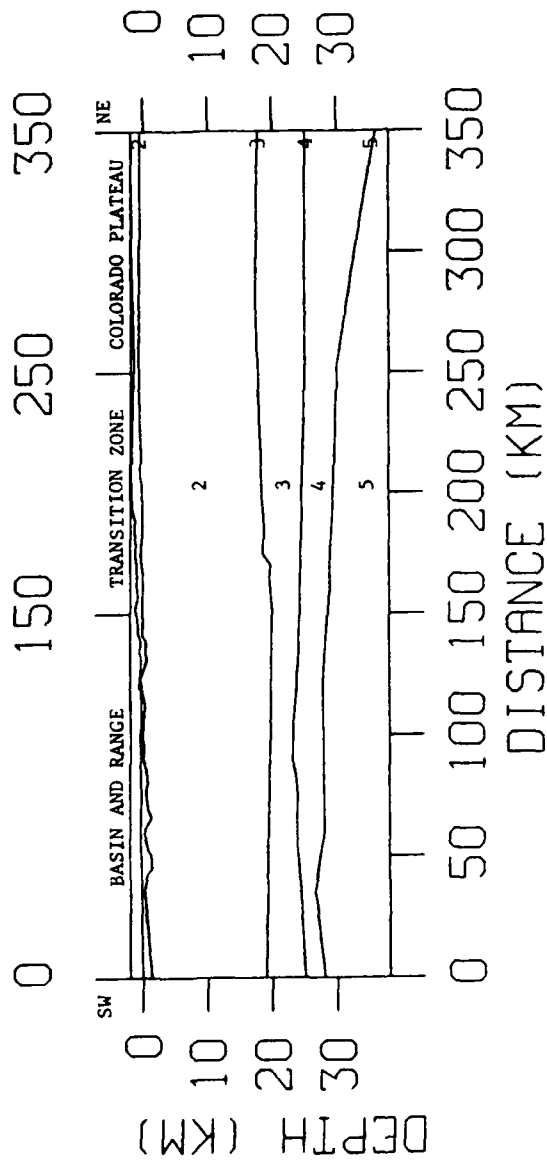


Figure 9. AGL Model of the Southern Basin and Range, the Transition Zone, and the Colorado Plateau. The datum is sea level. Shot point 15 (SH20) is located at 0 and shot point 34 (SH17) is near 350 km on the model. Weak deep reflections and lack of deep refracted arrivals from the Colorado Plateau resulted in poor resolution of the structure in that province below the thick upper crustal layer (see ray paths in Figure 15). The crustal thickness shown for the northeast end of the model was taken from a depth to Moho map.<sup>12</sup> Velocity gradients, average velocities, and Poisson's ratios can be found in Tables 7b and 7c.

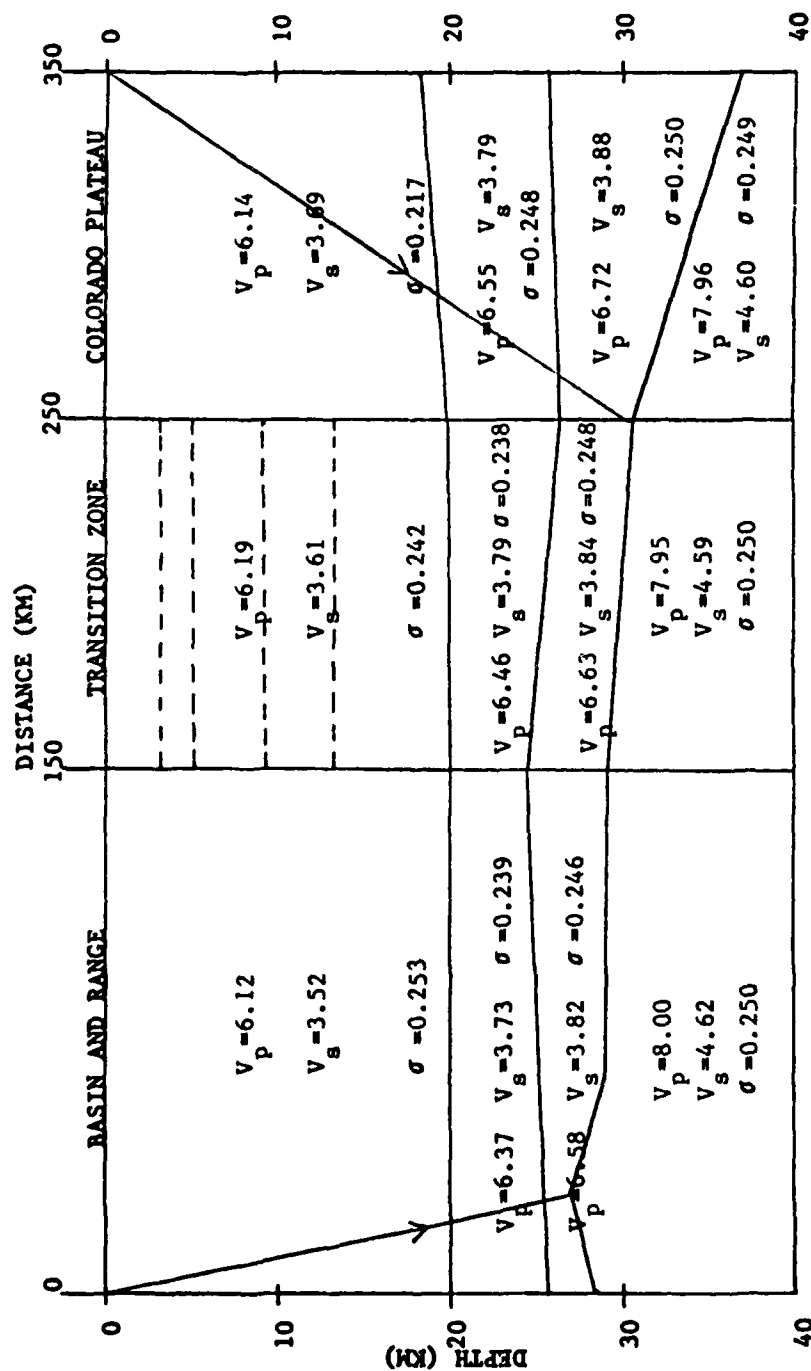


Figure 10. Cartoon Drawing of the Velocity Structure and Poisson's Ratios of the AFGL Model. Velocities are in kilometers per second. The crust was sampled along ray paths in the area between the arrows. Velocities in the deeper layers of the Colorado Plateau are not well defined by this data set. Reflective surfaces in the upper crust of the Transition Zone are indicated by dotted lines because velocities for the individual layers were not determined.

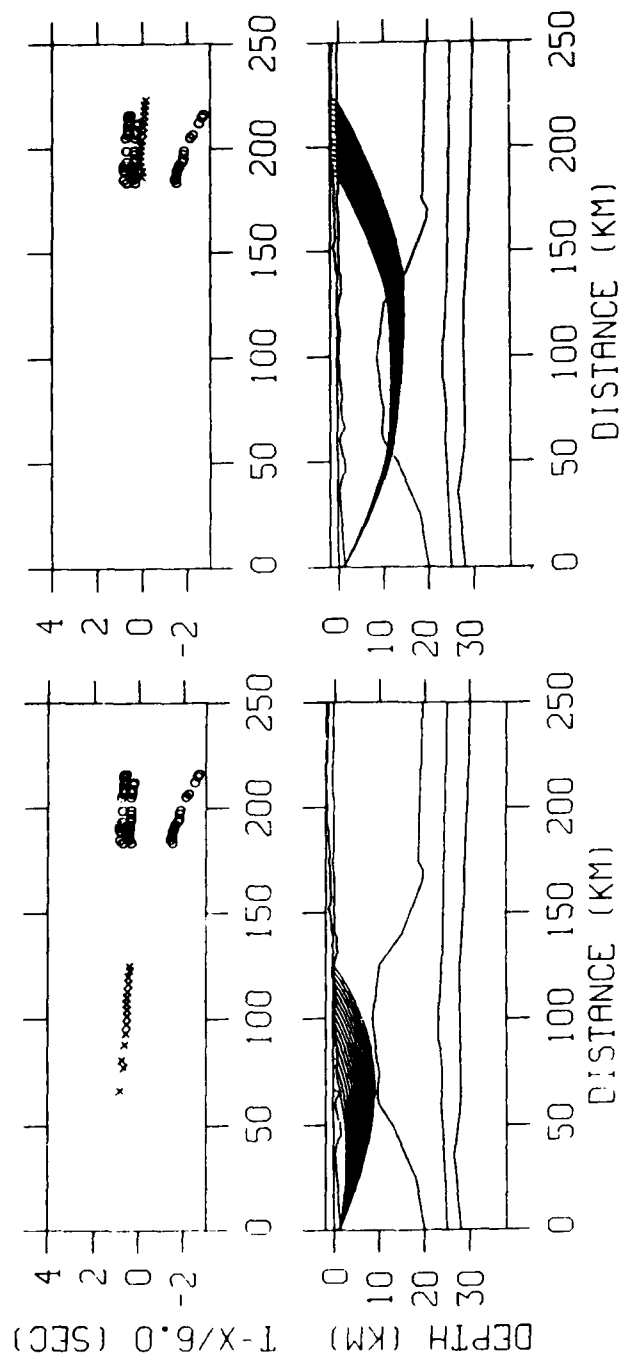


Figure 11. Raytracing from Shot Point 20 (SH15) Through the USGS Crustal Structure. The ray traces that rays directed through the structure arrive about 0.5 sec earlier than arrivals observed around 1 sec reduced travel time. The symbol for a theoretical reflected arrival is X, for a theoretical reflected arrival is +, and for an observed arrival is 0. (a) Refractions through layer 2 do not appear to reach the AFGL stations (b) Refractions through layer 3 are about 1 second earlier than observed high amplitude arrivals.

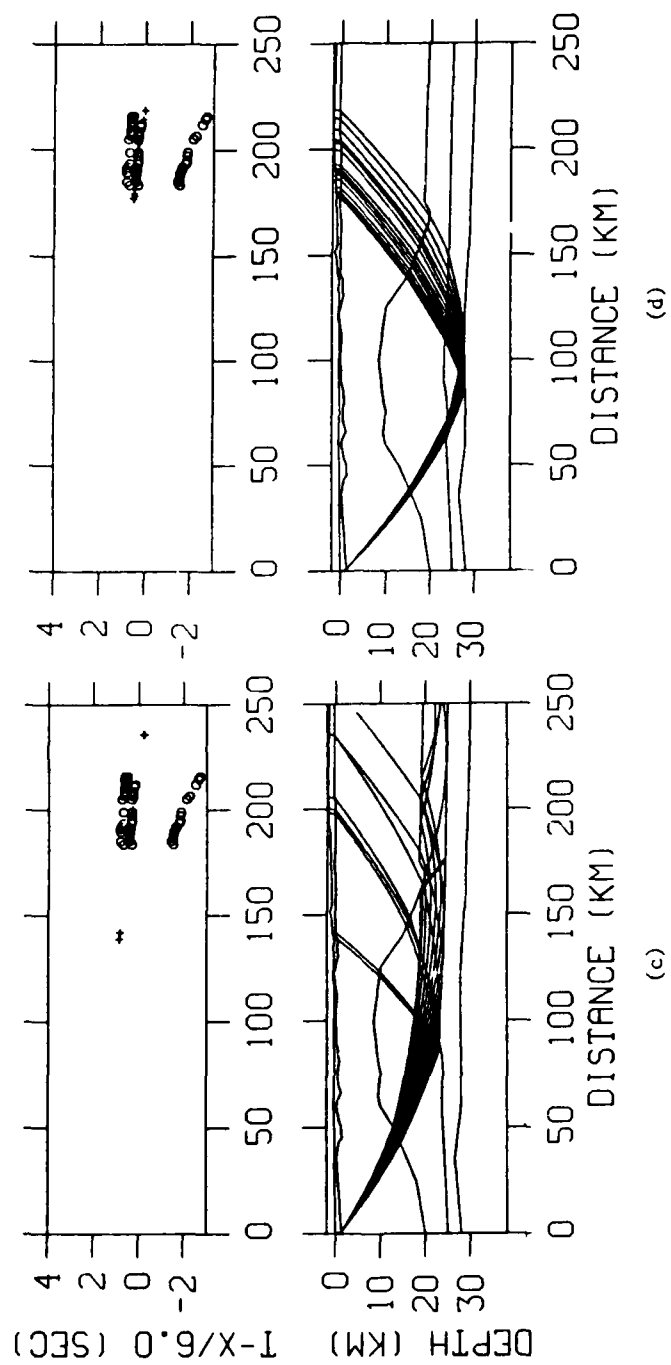


Figure 11. (c and d) Reflections from interface 4 and reflections from interface 5 (Moho) arrive before the observed reflections at about 1 s reduced travel time.

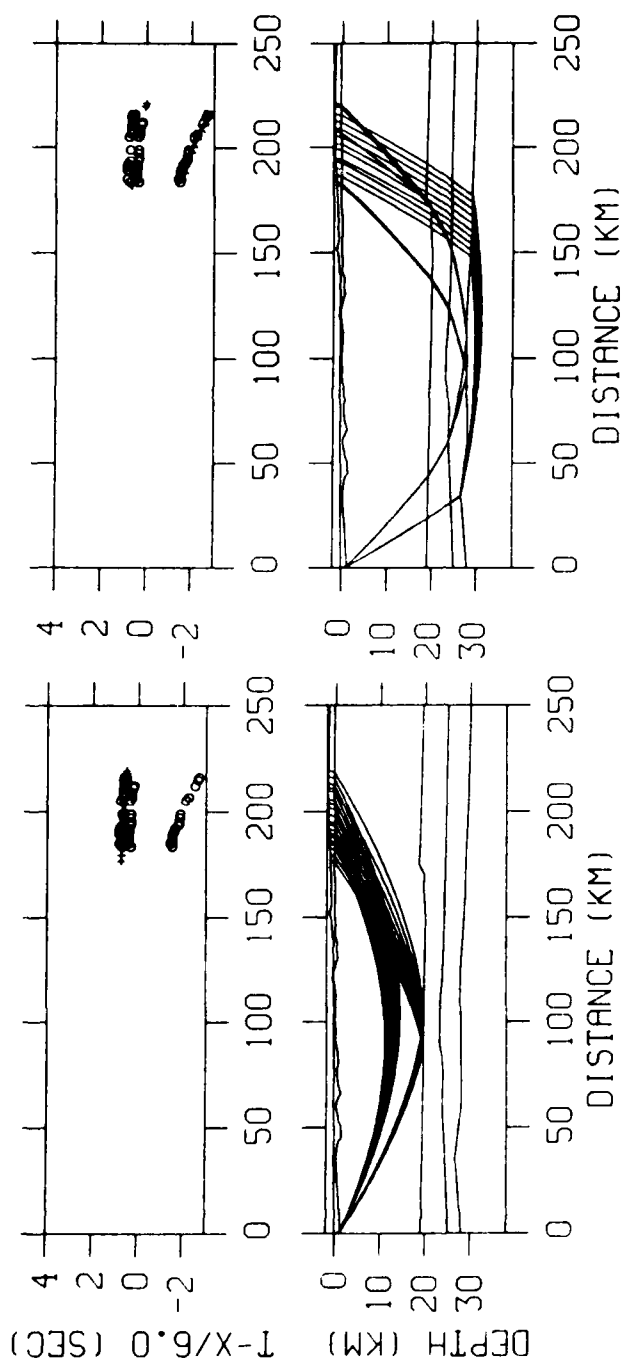


Figure 12. Raytracing from Shot Point 20 (SH115) Through the AFGL Crustal Structure. This model of the Basin and Range shows that flattening the USGS interface 3 allows (a) refractions through layer 2 and reflections off interface 3 to arrive at observed travel times about 1 s reduced travel time (b) reflections off the Moho to arrive at expected times between 0 to 1 s reduced travel time. The symbols are the same as those in Figure 11.

The AFGL Transition Zone model (Figure 9) has a thin 1 - 2 km surficial layer with a P velocity of 2.71 - 3.6 km/s. The upper crustal layer has a velocity of 6.06 - 6.31 km/s and is 18 - 20 km thick. Layer 3 is 5 - 7 km thick and has a P velocity of 6.37 - 6.55 km/s. Layer 4 is 4 - 5 km thick with a velocity of 6.58 - 6.68 km/s. The Moho discontinuity appears to be 28 - 31 km deep, dipping toward the northeast.  $P_n$  for the Transition Zone is 8.0 km/s. Several shallow crustal layers within the upper crust (layer 2) are indicated in the AFGL data, supporting the interpretation by McCarthy and others.<sup>3</sup> They can also be seen in Figure 4 in the results of Hauser and others.<sup>11</sup> The interfaces for these layers are estimated to be at depths of 3, 9, 11, and 13 km. These shallow interfaces are indicated in the cartoon drawing in Figure 10.

The surficial layer of the AFGL Colorado Plateau model is about 2 km thick with a P-wave velocity of 2.68 - 3.80 km/s. The upper crustal layer is about 18 km thick and has a P velocity of 6.06 - 6.22 km/s. The deeper layers are poorly resolved because the seismic records lack clear reflections and refractions from the deeper layers. Figure 13 shows the theoretical ray paths from the shots farthest to the northeast of the AFGL stations and indicate the areas in the model where it is best resolved.

## 5.2 Shear Velocity Structure and Poisson's Ratio

As an aid in the interpretation of the shear-wave arrivals, the record sections were replotted assuming a Poisson's ratio of 0.25, meaning  $V_p/V_s = 1.73$ . For this study the compressional-wave record sections were plotted with a reducing velocity of 6 km/s and a time scale of 1 s per time division. The shear-wave record sections were plotted with a reducing velocity of 6.00 km/s divided by 1.73 and a time scale of 1 s times 1.73 per time division. When the shear-wave record section plotted at the ratio of 1.73 is placed over the compressional wave record section for the same event, the first P-wave arrival to a particular station should lie directly beneath the first S-wave arrival to the same station if Poisson's ratio is 0.25. If the S arrival is earlier or later than expected, a deviation in Poisson's ratio from 0.25 is indicated. An additional aid in picking shear arrivals from unfiltered records containing a high proportion of high frequencies was the existence of an apparent increase in the low frequencies at the onset of the Sg phase.

Raytracing was used to develop the shear velocity structure presented in Table 7b and 7c, and in the cartoon drawing of the structures of the southern Basin and Range, the Colorado Plateau, and the Transition Zone in Figure 10. The initial crustal model used in the analysis of the shear velocity structure was the AFGL model described above. Assuming a Poisson's ratio of 0.25, the values of the AFGL P-wave velocity structure were divided by 1.73 to determine the starting S-wave velocity structure.

The north-south horizontal-component records were used in the raytracing analysis. In a station-by-station comparison, the average variance for the first S arrivals among the seismograms from each of the three components was 0.0082 s. This value indicates that any deviation due to anisotropy is very small and permits raytracing to be done with travel times from any of the three components. The horizontal-component seismograms displayed more prominent shear arrivals than the vertical-component records, and since the north-south component records showed fewer instrument failures, that component was chosen for the analysis.



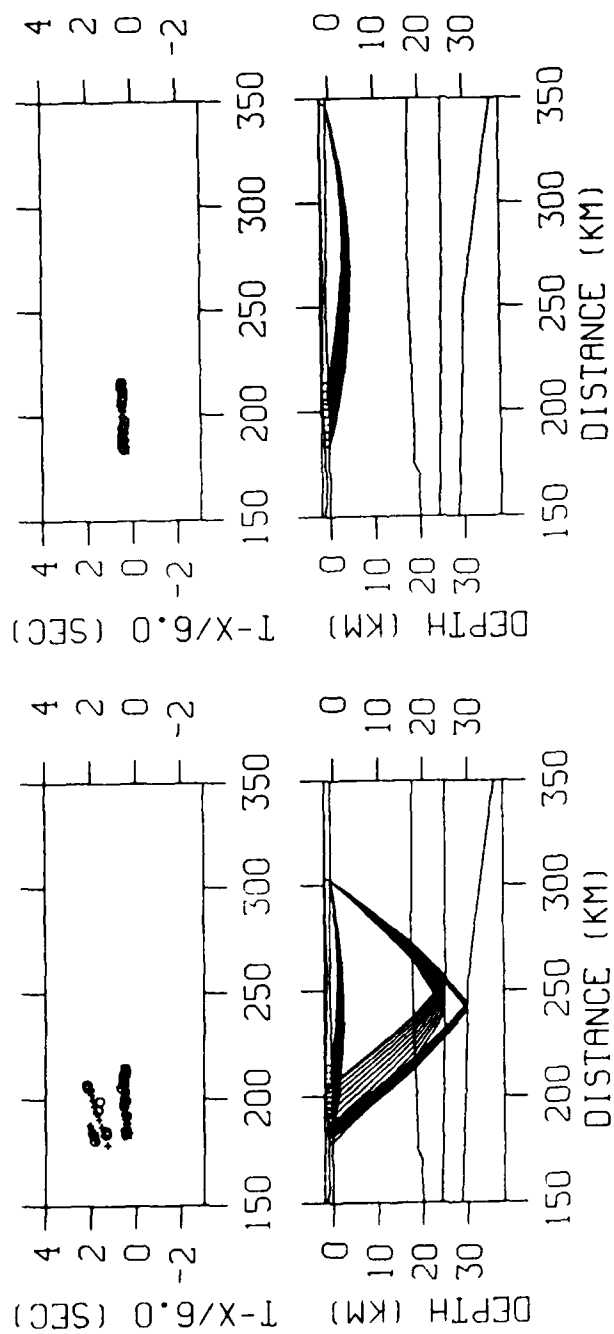


Figure 13. Theoretical Ray Paths through the AFGCL Model from Shots in the Colorado Plateau. (a) shot point 33 (SH22): reflections from interface 4 and 5 (Moho) appear to reflect near the Transition Zone-Colorado Plateau border (around 150 km) (b) shot point 34 (SH117): upper crustal refractions through layer 2 are shown. The symbols are the same as those in Figure 11.

Shear-wave velocities increase from the Basin and Range toward the northeast except for the upper mantle shear velocity  $S_n$  which is 4.59 km/s in the Transition Zone and 4.62 km/s in the Basin and Range. The velocities found for the Colorado Plateau, with the exception of  $S_g$ , are poorly resolved due to a lack of strong reflections from deep interfaces (4,5) and to the absence of  $S_n$  in the seismograms from the shots to the northeast. The paths of theoretical rays from the shots farthest to the northeast are shown in Figure 13. Velocity resolution below and to the northeast of these raypaths is poor.

Estimates of Poisson's ratio are an important result of determining both P and S velocity models. Because Poisson's ratio is sensitive to such variables as quartz content<sup>63</sup> and the presence of fluids,<sup>64,65</sup> it can be used to put constraints on possible chemical or mineral compositions of subsurface materials. To calculate Poisson's ratios, the top and bottom velocity values of velocity ranges for each province were averaged. The calculated constant velocities for the layers were then used in the formula:

$$\sigma = \frac{1}{2} \left[ 1 - \left[ \left( \frac{V_p}{V_s} \right)^2 - 1 \right]^{-1} \right]$$

Where  $V_p$  is the compressional velocity and  $V_s$  is the shear velocity of the layer.

Plots in Figures 14, 15, and 16 point out deviations in Poisson's ratio. A very low Poisson's ratio was found in the thick upper crustal layer in the Colorado Plateau from  $P_g$  and  $S_g$  velocities. Graphical evidence for this variation can be seen in Figure 14. Low Poisson's ratios indicate a quartz-rich granitic/gneissic composition<sup>66</sup> or the presence of fluids at low pore pressures and temperatures of 200°C - 300°C.<sup>65</sup> There is no resolution on Poisson's ratio for layers deeper than layer 2 in the Colorado Plateau.

Figure 15 shows evidence of a Poisson's ratio slightly lower than 0.25 in the upper crust of the southern Basin and Range, as was also suggested by Warren.<sup>12</sup> The same figure indicates a Poisson's ratio very near to 0.25 using the later arrivals from layers beneath the upper crust. Figure 16 presents additional evidence that Poisson's ratio in the deeper layers (4,5) of the northern part of the southern Basin and Range are not as high as reported for the northern Basin and Range<sup>7,9,67</sup> or for the southern Basin and Range.<sup>9</sup> High Poisson's ratios indicate mafic or quartz-poor composition.<sup>66</sup> This study

- 
63. Kern, H. (1982) Elastic-Wave Velocity in Crustal and Mantle Rock at High Pressure and Temperature: The Role of the High-Low Quartz Transition and of Dehydration Reactions, *Phys. Earth Planet. Inter.* **9**:12-23.
  64. Nur, A. and Simmons, G. (1969) The Effect of Saturation on Velocity in Low Porosity Rocks, *Earth Planet. Sci. Ltrs.* **7**:183-193.
  65. Spencer, J.W. and Nur, A. (1976) The Effect of Pressure, Temperature, and Pore Water on Velocities in Westerly Granite, *J. of Geophys. Res.* **81**:899-904.
  66. Holbrook, S.W., Gajewski, D., and Prodehl, C. (1987) Shear-Wave Velocity and Poisson's Ratio Structure of the Upper Lithosphere in Southwest Germany, *Geophys. Res. Ltrs.* **14**(No. 3):231-234.
  67. Clement, W.P., Holbrook, W.S., Catchings, R.D., and Mooney, W.D. (1987) Determination of Average Crustal Poisson's Ratio for Northern Nevada from Vertical Recording of SmS, EOS Transactions, *Amer. Geophys. Union* **68**(44).

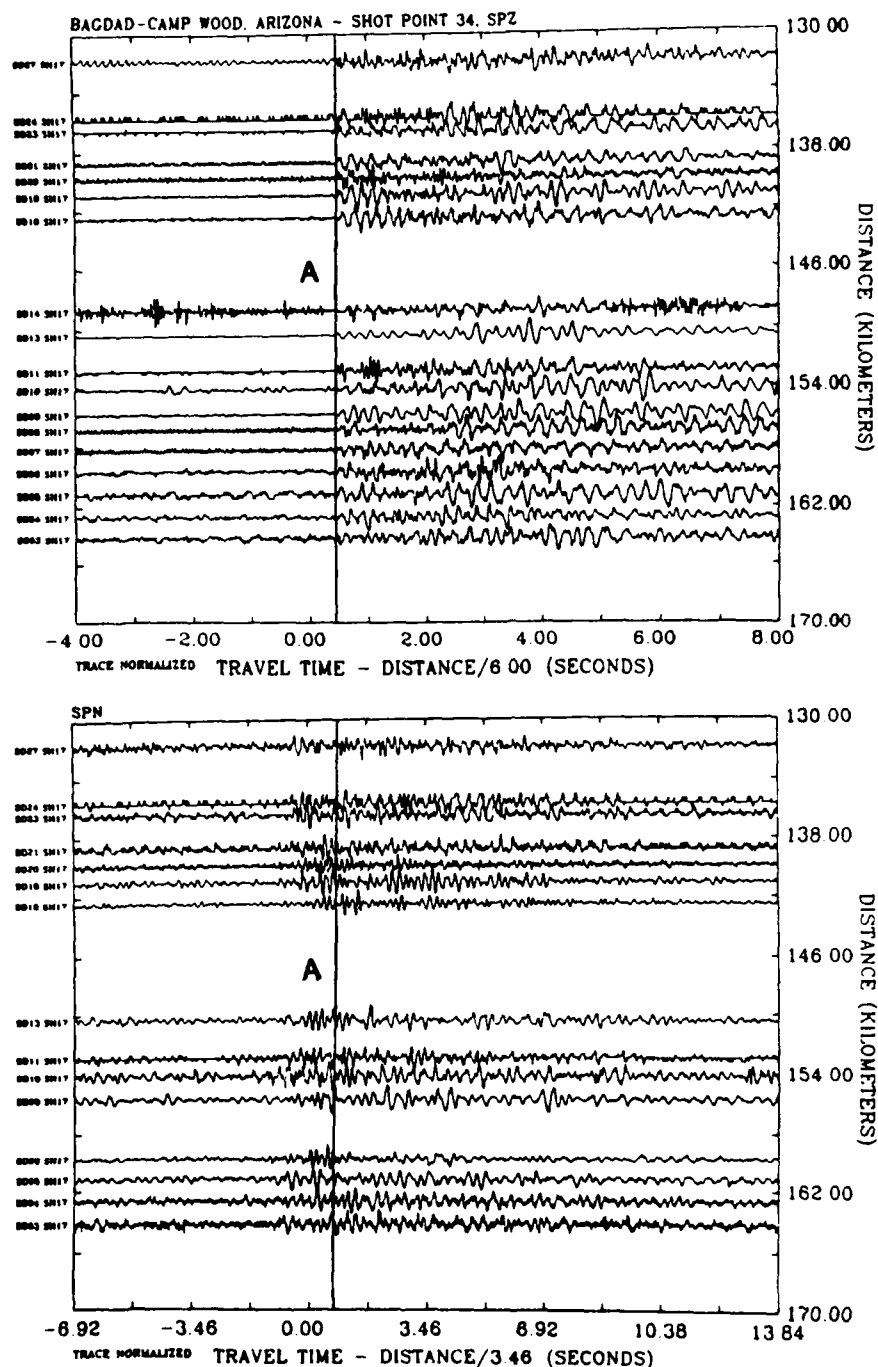


Figure 14. Comparison of P and S Velocities in the Upper Crust of the Colorado Plateau. Upper plot is a compressional-wave seismic record and lower plot is a shear-wave seismic record for shot point 34 (SH17). Reference line A approximates  $P_g$  in upper plot. If Poisson's ratio were 0.25,  $S_g$  in lower plot would also fall on reference line A. Early shear first arrivals in lower plot indicate a low Poisson's ratio in the upper crust of the Colorado Plateau.

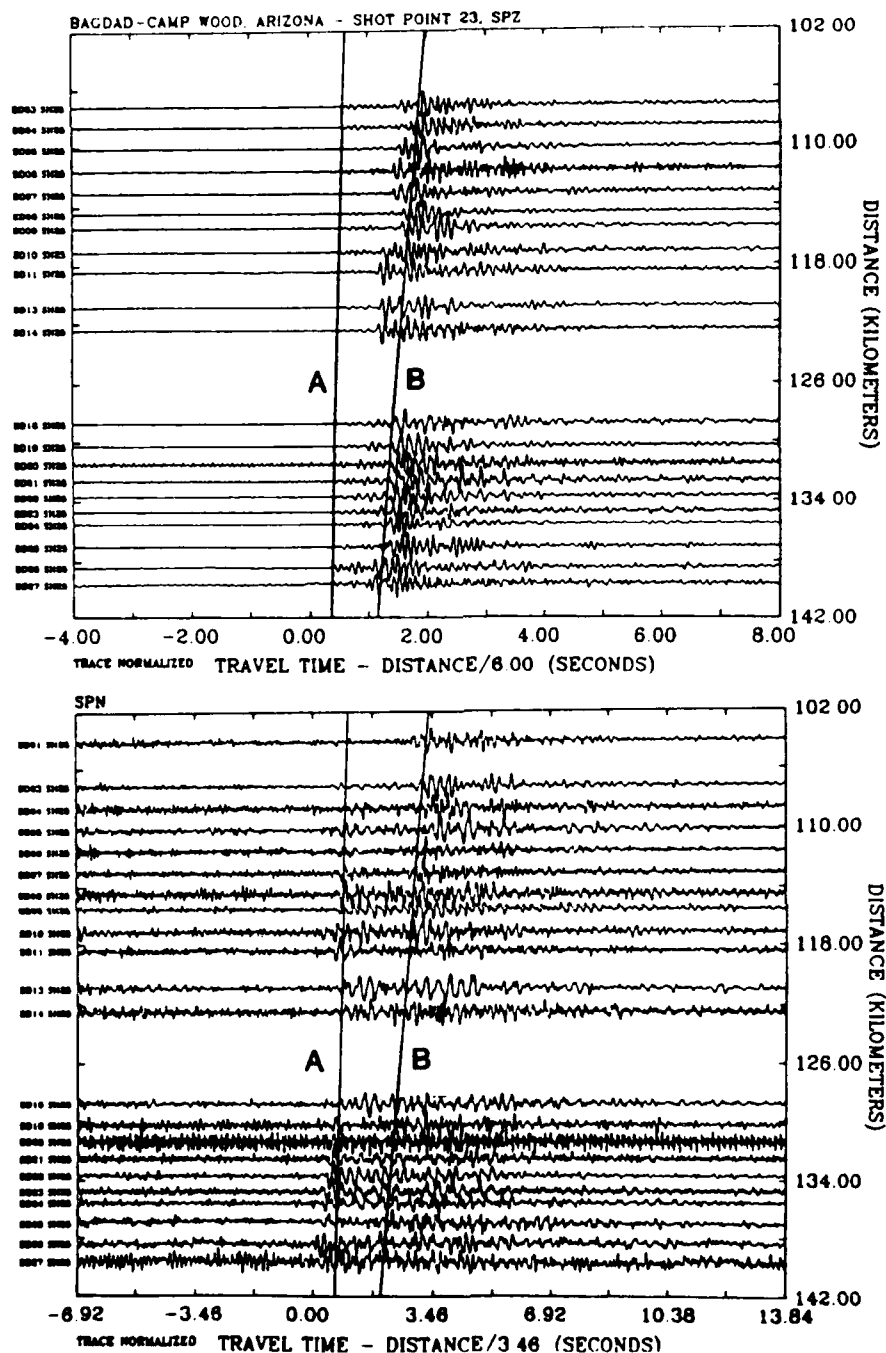


Figure 15. Comparison of P and S Velocities in the Upper Crust of the Basin and Range. Upper plot is a compressional-wave seismic record and lower plot is a shear-wave seismic record for shot point 23 (SH25). Upper crustal refracted S arrivals near reference line A appear to arrive slightly earlier than P arrivals in the Basin and Range. P and S reflections from deep layers appear to be in the ratio 1.73 as seen by reference line B. This indicates a Poisson's ratio near 0.25 for the lower crust and upper mantle.

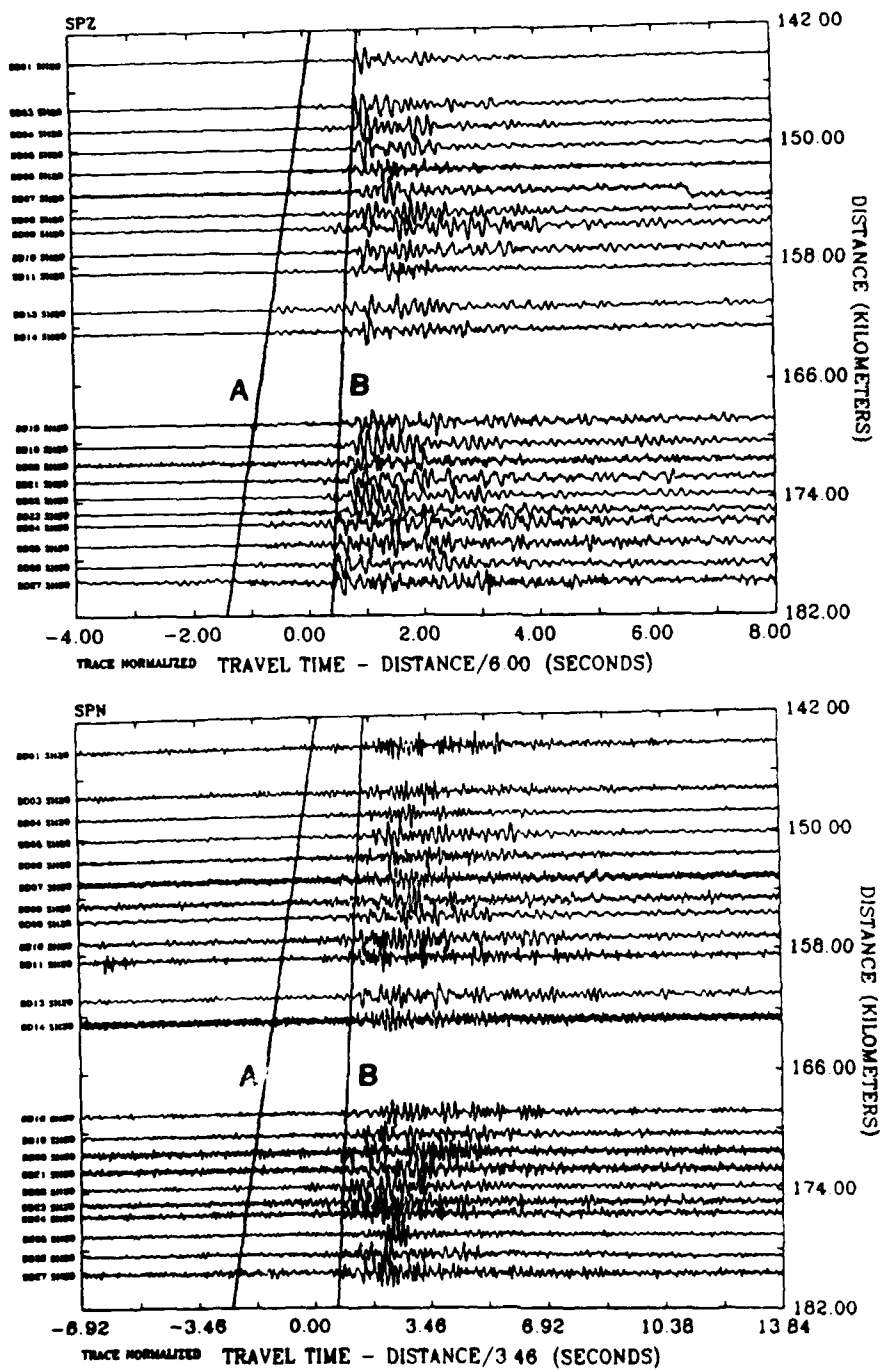


Figure 16. Comparison of P and S Velocities in the Lower Crust of the Basin and Range. Upper plot is a compressional-wave seismic record and lower plot is a shear-wave seismic record for shot point 20 (SH15). A station-to-station comparison can be made using reference lines A and B. Shear and compressional arrivals for the same phase are in the ratio 1.73 indicating that Poisson's ratio approximates 0.25 in the lower layers of the southern Basin and Range.

suggests that the composition of the deeper layers of the southern Basin and Range may be different than the composition of the deeper layers of the northern Basin and Range.

Considering the error associated with the velocity results, the crustal and upper mantle velocities developed in this study are comparable with past studies in the area with the exception of the lower Pn value of 7.67 km/s of Sinno and others.<sup>1</sup> It is stated by Sinno and others<sup>1</sup>, however, that their Pn velocity is possibly that of a layer above the Moho discontinuity. Because Pn was not seen as a first arrival in the records from the Colorado Plateau, the thickness of the crust in that province is estimated to be a minimum of 31 km. The thickness of the crust in the southern Basin and Range and the Transition Zone, 26.5 - 28±1 km and the 28 - 31±1 km, respectively, fall within the error ranges of past studies in the area except for that of Hauser and others.<sup>13</sup> COCORP crustal thickness in the northeast part of the Transition Zone is shown (near Camp Wood in Figure 4) to be about 36 km, 4 km thicker than that found in this study for the same area.<sup>13</sup>

## 6. CONCLUSIONS

The purpose of this study was to develop compressional wave and shear-wave velocity structures and then to calculate the resulting Poisson's ratios for the southern Basin and Range, the Colorado Plateau, and the Transition Zone in northwestern Arizona. Raytracing was the principal method used in the study. The raytracing analysis was begun with a USGS crustal P velocity structure model developed from USGS Pacific Arizona Crustal Experiment data. The USGS crustal model was modified in three ways: (1) Interface 3 of the 5 layer USGS model, in the southern Basin and Range Province as modified to make layer 3 a 3 - 5 km thick layer in place of the USGS anticlinal feature which thickened to about 10 km in the center of the 150 km profile. This alteration gives layer 2 a thickness of 18 - 20 km, extending across both Provinces and the Transition Zone. (2) Several additional shallow layers were included in the upper 20 km of the Transition Zone in the AFGL model. Estimated depths of the layers are 3, 9, 11, and 13 km. (3) The USGS model was extended 100 km into the Colorado Plateau.

Crustal thicknesses in the AFGL model range from 26.5 - 28 km in the southern Basin and Range to 28 - 31 km in the Transition Zone. Depth to the Moho could not be determined in the Colorado Plateau because of lack of clear deep reflections and refractions.

Resulting P and S velocity structures are compatible with previous studies in the area. In the Transition Zone, where the AFGL stations were located, upper crustal velocities Pg and Sg are 6.19 km/s and 3.60 km/s, respectively. Mid-crustal velocities for layers 3 and 4 are 6.46 and 3.79 km/s for P<sub>3</sub> and S<sub>3</sub>, and 6.63 and 3.84 km/s for P<sub>4</sub> and S<sub>4</sub>. Upper mantle velocities, Pn and Sn, are 7.95 km/s and 4.59 km/s. Poisson's ratios in the Transition Zone approach 0.25 except for that of layer 3 which is 0.238.

P and S velocities above the Moho discontinuity in the southern Basin and Range are slightly lower than those of the Transition Zone. Pg and Sg are 6.12 km/s and 3.52 km/s, respectively. Velocities of layer 3 are 6.37 km/s and 3.73 km/s. Layer 4 velocities are 6.58 km/s and 3.82 km/s. Upper mantle velocities appear to increase toward the southwest. Pn and Sn are 8.0 km/s and

4.62 km/s, respectively. A low Poisson's ratio of 0.239 was found in layer 3 of the Basin and Range Province. Poisson's ratios of the other layers approach 0.25.

Records from the Colorado Plateau direction display weak Moho reflections, possibly indicating a strong velocity gradient at that discontinuity.<sup>68,69</sup> The PACE shot farthest to the northeast in the Colorado Plateau apparently was not distant enough to observe Pn as a first arrival. Clear Pg and Sg arrivals in the records resulted in P and S velocities of 6.14 km/s and 3.69 km/s, respectively. A low Poisson's ratio of 0.217 was calculated for this 19 - 20 km thick layer suggesting the presence of fluids<sup>64,65</sup> or that the material of the upper crust has a high quartz content.<sup>63,66</sup> The lack of clear reflections and refractions from layers deeper than 20 km resulted in poor resolution of velocities or structure below that depth.

---

68. Melssner, R. (1973) Moho as a Transition Zone, *Geophys. Surveys* 1(2):195-216.

69. Fuchs, K. (1969) On the Properties of Deep Crustal Reflectors, *Zeitschrift Für Geophysik* 35:133-149.

## References

1. Sinno, Y.A., Keller, G.R., and Sbar, M.L. (1981) A Crustal Seismic Refraction Study in West-Central Arizona, *J. of Geophys. Res.* **86**(B6):5023-5038.
2. Thompson, G.A., and Zoback, M.L. (1979) Regional Geophysics of the Colorado Plateau, *Tectonophysics* **61**:149-181.
3. Chronic, H. (1986) *Roadside Geology of Arizona*, Mountain Press Publishing Company, Missoula, MT, 340p.
4. McCarthy, J., Fuis, G.S., and Wilson, J. (1987) Crustal Structure of the Whipple Mountains, Southeastern California: A Refraction Study Across a Region of Large Continental Extension, *Geophys. J.R. Astr. Soc.* **89**:119-124.
5. McCarthy, J., Fuis, G.S., Wilson, J., McKissick, C., and Larkin, S. (1987) PACE Seismic Refraction and Wide-Angle Reflection Data Recorded Across the Central Arizona Transition Zone, *EOS Transactions* **68**(44):1359.
6. Braille, L.W., Smith, R.B., Keller, G.R., and Welch, R.M. (1974) Crustal Structure Across the Wasatch Front from Detailed Seismic Refraction Studies, *J. of Geophys. Res.* **79**(17):2669-2677.
7. Keller, G.R., Smith, R.B., and Braille, L.W. (1975) Crustal Structure Along the Great Basin-Colorado Plateau Transition from Seismic Refraction Studies, *J. of Geophys. Res.* **80**:1093-1098.
8. Roller, J.C. (1965) Crustal Structure in the Eastern Colorado Plateaus Province from Seismic-Refraction Measurements, *Bull. of the Seismolog. Soc. of Amer.* **55**(No. 1):107-119.
9. Bache, T.C., Rodi, W.L., and Harkrider, D.G. (1978) Crustal Structures Inferred from Rayleigh-Wave Signatures of NTS Explosions, *Bull. of the Seismolog. Soc. of Amer.* **68**(No. 5):1399-1413.
10. Langston, C.A. and Helmberger, D.V. (1974) Interpretation of Body and Rayleigh Waves from NTS to Tucson, *Bull. of Seismolog. Soc. of Amer.* **64**(6):1919-1929.
11. Diment, W.H., Stewart, S.W., and Roller, J.C. (1961) Crustal Structure from the Nevada Test Site to Kingman, Arizona, from Seismic and Gravity Observations, *J. of Geophys. Res.* **66**(1):201-213.
12. Warren, D.H. (1969) A Seismic-Refraction Survey of Crustal Structure in Central Arizona, *Geolog. Soc. of Amer. Bull.* **80**:257-282.



13. Hauser, E.C., Gephart, J., Latham, T., Oliver, J., Kaufman, S., Brown, L., and Lucchitta, I. (1987) COCORP Arizona Transect: Strong Crustal Reflections and Offset Moho Beneath the Transition Zone, *Geology* **15**:1103-1106.
14. Hauser, E.C. and Lundy (1988) COCORP Deep Reflections: Moho at 50 km (16 s) Beneath the Colorado Plateau, in review for *J. of Geophys. Res.*
15. King, P.B. (1969) The tectonics of North America - A Discussion to Accompany the Tectonic Map of North America, scale 1:5,000,000: U.S. Geological Survey Prof. Paper 268, 95p.
16. Stewart, J.H. (1978) Basin-Range Structure in Western North America, A Review, *Geol. Soc. of Amer. Mem.* **152**:1-30.
17. Allmendinger, R.W., Hauge, T.A., Hauser, E.C., Potter, C.J., Klemperer, S.L., Nelson, K.D., Knuepfer, P., and Oliver, J. (1987) Overview of the COCORP 40 degree N Transect, Western United States: The Fabric of an Orogenic Belt, *Geol. Soc. of Amer. Bull.* **98**:308-319.
18. Burchfiel, B.C. and Davis, G.A. (1972) Structural Framework and Evolution of the Southern Part of the Cordilleran Orogen, Western United States, *Amer. J. of Sci.* **272**:97-118.
19. Burchfiel, B.C. and Davis, G.A. (1975) Nature and Controls of the Cordilleran Orogenesis, Western United States - Extensions of an Earlier Synthesis, *Amer. J. of Sci.* **275-A**:275.
20. Stewart, J.H. and Poole (1974) Lower Paleozoic and Uppermost Precambrian Cordilleran Miogeocline, Great Basin, Western United States, In Dickinson, W.R., ed., *Tectonics and Sedimentation*, Soc. of Econ. Paleontology and Mineralog. Spec. Pub. **22**:28-57.
21. Stewart, J. H. (1972) Initial Deposits in the Cordilleran Geosyncline: Evidence of a Late Precambrian (< 850 m.y.) Continental Separation, *Geol. Soc. of Amer. Bull.* **83**:1345-1360.
22. Canadian Geological Survey (1970) Geologic Map of Canada in Douglas, R.J.W., *Geology and Economic Minerals of Canada*, Canada Geologic Survey Economic Geology Report 1, Scale 1:5,000,000.
23. Comite de la Carta Geologica de Mexico (1968) Carte Geologica de la Republica Mexicana, Scale 1:2,000,000.
24. Lopez-Ramos, E. (1969) Marine Paleozoic Rocks of Mexico, *Amer. Assoc. of Petrol. Geol. Bull.* **53**:2399-2417.
25. King, P.B. and Beikman, H.M. (1974) Geologic Map of the United States, U.S. Geological Survey Map, Scale 1:2,500,000.
26. Gastil, R.G., Phillips, R.P., and Allison, E.C. (1975) Reconnaissance Geology of the State of Baja California, *Geol. Soc. of Amer. Mem.* **140**:170.
27. Nicholas, R.L. and Rozendal, R.A. (1975) Subsurface Positive Elements within Ouachita Foldbelt in Texas and Their Relation to Paleozoic Cratonic Margin, *Amer. Assoc. of Petrol. Geol. Bull.* **59**:193-216.
28. Roberts, R.J., Hotz, P.E., Gilluly, J., and Ferguson, H.G. (1958) Paleozoic Rocks of North-Central Nevada, *Amer. Assoc. of Petrol. Geol. Bull.* **42**:2813-2857
29. Speed, R.C. (1982) Evolution of the Sialic Margin in Central Western United States, in Watkins, J. and D. Drake eds., *Geology of Continental Margins*, *Amer. Assoc. of Petrol. Geol. Mem.* **34**:457-468.
30. Bates, R.L. and Jackson, J.A. eds. (1984) *Dictionary of Geological Terms*, Anchor Press/Doubleday, NY, 3rd ed.
31. Siberling, N.J. and Roberts, R.J. (1962) Pretertiary Stratigraphy and Structure of Northwestern Nevada, *Geol. Soc. of Amer. Spec. Paper* **72**:1-50
32. Speed, R.C. (1979) Collided Paleozoic Microplate in the Western United States, *J. of Geol.* **87**:279-292.
33. Schweichert, R.A. and Cowan, D.S. (1975) Early Mesozoic Tectonic Evolution of the Western Sierra Nevada, California, *Geol. Soc. of Amer. Bull.* **86**:1329-1336.
34. Schweichert, R.A. (1981) Tectonic Evolution of the Sierra Nevada Range, in Ernst, W.G. ed., *The Geotectonic Development of California*, Englewood Cliffs, New Jersey, Prentice-Hall, p87-131.

35. Nelson, K.D., Zhu, T.F., Gibbs, A., Harris, R., Oliver, J.E., Kaufman, S., Brown, L.D., and Schweichert, A. (1985) COCORP Deep Seismic Reflection Profiling in the Northern Sierra Nevada, California, *Tectonics* **5**:321-333.
36. Hamilton, W. (1969) The Volcanic Central Andes - A Modern Model for the Cretaceous Batholiths and Tectonics of Western North America, *Oregon Dept. of Geolog. and Miner. Indus. Bull.* **65**:175-184.
37. Coney, P.J. (1978) Mesozoic-Cenozoic Cordilleran Plate Tectonics, in Smith, R.B. and Eaton, G.P. Eds., *Cenozoic Tectonics and Regional Geophysics of the Western Cordillera*, *Geolog. Soc. of Amer. Mem.* **152**:33-50.
38. Dickenson, W.R. and Snyder, W.S. (1978) Plate Tectonics of the Laramide Orogeny, In Mathews, V. Ed., *Laramide Folding Associated with Basement Block Faulting in the Western United States*, *Geolog. Soc. of Amer. Mem.* **151**:355-366
39. Chen, J.H. and Moore, J.G. (1982) Uranium-lead isotopic ages from the Sierra Nevada Batholith, California, *J. of Geophys. Res.* **87**:4761-4784.
40. Hintze, L.F. (1973) Geologic History of Utah, *Brigham Young Univ. Geology Studies* **25**:181.
41. Miller, C.F. and Bradfish, L.J. (1980) An inner Cordilleran Belt of Muscovite-Bearing Plutons, *Geology* **8**:412-416.
42. Stewart, J.H. (1980) Geology of Nevada, *Nevada Bur. of Mines and Geology Spec. Pub.* **4**:136.
43. Zoback, M.L. and Thompson, G.A. (1978) Basin and Range Rifting in Northern Nevada: Clues from a Mid-Miocene Rift and its Subsequent Offsets, *Geology* **6**:111-116.
44. Zoback, M.L., Anderson, R.E., and Thompson, G.A. (1981) Cainozoic Evolution of the State of Stress and Style of Tectonism of the Basin and Range Province of the Western United States, *Roy. Soc. of London Philosop. Trans.* **A-300**:407-434.
45. Davis, G.H. and Coney, P.J. (1979) Geologic Development of the Cordilleran Metamorphic Core Complexes, *Geology* **7**:120-124.
46. Crittenden, M.D. Jr., Coney, P.J., and Davis, G.H., Eds. (1980) Cordilleran Metamorphic Core Complexes, *Geolog. Soc. of Amer. Mem.* **153**:490.
47. Armstrong, R.L. (1982) Cordilleran Metamorphic Core Complexes - from Arizona to Southern Canada, *Annual Rev. of Earth and Planet. Sci.* **10**:129-154.
48. Armstrong, R.L. (1972) Low Angle (Denudation) Faults Hinterland of Sevier Orogenic Belt, Eastern Nevada and Western Utah, *Geolog. Soc. of Amer. Bull.* **83**:1729-1754.
49. Proffett, J.M., Jr. (1977) Cenozoic Geology of the Yerrington District, Nevada, and Implications for the Nature and Origin of Basin and Range Faulting, *Geolog. Soc. of Amer. Bull.* **88**:247-266.
50. McKee, E.H. (1971) Tertiary Igneous Chronology of the Great Basin of Western United States, Implications for Tectonic Models, *Geolog. Soc. of Amer. Bull.* **82**:3497-3502.
51. Christiansen, R.L. and Lipman, P.W. (1972) Cenozoic Volcanism and Plate-Tectonic Evolution of the Western United States II, Late Cenozoic, *Roy. Soc. of London Philosop. Trans.* **271**:249-284.
52. Noble, D.C. (1972) Some Observations on the Cenozoic Volcano-Tectonic Evolution of the Great Basin, Western United States, *Earth and Planet. Sci. Let.* **17**:142-150.
53. McBirney, A.R., Sutter, J.F., Naslund, H.R., Sutton, K.G., and White, C.M. (1974) Episodic Volcanism in the Central Oregon Cascade Range, *Geology* **2**:585-589.
54. Best, M.G. and Brimhall, W.H. (1974) Late Cenozoic Alkaline Basaltic Magmas in the Western Colorado Plateaus and the Basin and Range Transition Zone, USA and their Bearing on Mantle Dynamics, *Geolog. Soc. of Amer. Bull.* **85**:1677-1690.
55. Prodehl, C. (1970) Seismic Refraction Study of Crustal Structure in the Western United States, *Geolog. Soc. of Amer. Bull.* **81**(9):2629-2646.
56. Toppozada, T. and Sanford, A.R. (1976) Crustal Structure in Central New Mexico Interpreted from the Gasbuggy Explosion, *Bull. of the Seismolog. Soc. of Amer.* **66**(3):877-886.

57. Keller, G.R., Smith, R.B., Braile, L.W., Heaney, R., and Shurbet, D.H. (1976) Upper Crustal Structure of the Eastern Basin and Range, Northern Colorado Plateau, and Middle Rocky Mountains from Rayleigh Wave Dispersion, *Bull. of the Seismolog. Soc. of Amer.* **66**(3):869-876.
58. Wickens, A.J. and Pec, K. (1968) A Crust-Mantle Profile from Mould Bay, Canada, to Tucson, Arizona, *Bull. of the Seismolog. Soci. of Amer.* **58**(6):1821-1831.
59. Mueller, S. and Landisman, M. (1971) An Example of the Unified Method of Interpretation for Crustal Seismic Data, *Geophys. J. Roy. Astron. Soc.* **23**:365-371.
60. Mueller, G. and Mueller, S. (1972) A Crustal Low-Velocity Zone in Utah, *Geolog. Soc. Amer. Abstr. Programs* **4**:204
61. Beghoul, M.N. and Barazangi, M. (1988) Relatively High Pn Velocity Beneath the Colorado Plateau Constrains Uplift Models, *EOS Trans.* **69**(16):496.
62. Luetgert, J.H. (1988) Users Manual for RAY84/R83PLT Interactive Two-Dimensional Raytracing/Synthetic Seismogram Package, U.S. Geological Survey Open File Report No. 88-238, 52p.
63. Kern, H. (1982) Elastic-Wave Velocity in Crustal and Mantle Rock at High Pressure and Temperature: The Role of the High-Low Quartz Transition and of Dehydration Reactions, *Phys. Earth Planet. Inter.* **9**:12-23.
64. Nur, A. and Simmons, G. (1969) The Effect of Saturation on Velocity in Low Porosity Rocks, *Earth Planet. Sci. Ltrs.* **7**:183-193.
65. Spencer, J.W. and Nur, A. (1976) The Effect of Pressure, Temperature, and Pore Water on Velocities in Westerly Granite, *J. of Geophys. Res.* **81**:899-904.
66. Holbrook, S.W., Gajewski, D., and Prodehl, C. (1987) Shear-Wave Velocity and Poisson's Ratio Structure of the Upper Lithosphere in Southwest Germany, *Geophys. Res. Ltrs.* **14**(No. 3):231-234.
67. Clement, W.P., Holbrook, W.S., Catchings, R.D., and Mooney, W.D. (1987) Determination of Average Crustal Poisson's Ratio for Northern Nevada from Vertical Recording of SmS, *EOS Transactions, Amer. Geophys. Union* **68**(44).
68. Meissner, R. (1973) Moho as a Transition Zone, *Geophys. Surveys* **1**(2):195-216.
69. Fuchs, K. (1969) On the Properties of Deep Crustal Reflectors, *Zeitschrift Fur Geophysik* **35**:133-149.